Supporting Information

A dimethylgallium boryl complex and its methyllithium addition compound

Nicole Dettenrieder, Christoph Schädle, Cäcilia Maichle-Mössmer, Peter Sirsch, and Reiner Anwander

Institut für Anorganische Chemie, Universität Tübingen, Auf der Morgenstelle 18, D-72076 Tübingen, (Germany)

Table of Contents:

S2 Experimental data including NMR spectra and crystallographic data

S19 Chart showing complexes with B−Ga bonds

S20 Computational details

[$Me_2Ga\{B(NArCH)_2\}$] (2a) (Ar = C_6H_3-2,6-*i*Pr_2):

S21 Selected geometrical parameters and Cartesian coordinates

S23 3D representation of selected molecular orbitals (LUMO, HOMO, HOMO−1)

S24 Contour plot of the electron density and isosurface plots of the negative Laplacian

S25 3D representation of selected natural bond orbitals

S26 Potential energy surface scan and bond ellipticity profile

[$B(NArCH)_2]^-$ (1a) (Ar = C_6H_3-2,6-*i*Pr_2):

S27 Selected geometrical parameters and Cartesian coordinates

S29 Contour plots of the electron density and the negative Laplacian

[Ar′$Ga\{B(C_6F_5)_3\}$] (C) (Ar′ = C_6H_3-2,6-$Dipp_2$, Dipp = C_6H_3-2,6-*i*Pr_2):

S30 Selected geometrical parameters and Cartesian coordinates

S32 Contour plot of the negative Laplacian

S33 AIM charges and selected topological parameters for **2a**, **1a**, and **C**

S34 References

General Considerations. All operations were performed with rigorous exclusion of air and water, using standard Schlenk, high-vacuum, and glovebox techniques (MBraun 200B; <0.1 ppm O_2, <0.1 ppm H_2O). Hexane, pentane, and toluene were purified by using Grubbs columns (MBraun SPS, Solvent Purification System) and stored in a glovebox. Benzene-d_6 (99.5%) was received from Deutero GmbH and toluene-d_8 (99.5%) from euriso-top. All deuterated solvents were dried over NaK for a minimum of 48 h, and filtered through a filter pipette (Whatman) before use. $GaMe_3$ (98%) was used as purchased from Dockweiler GmbH. MeLi was received as a 1.6 M solution in diethylether from AcrosOrganics, transferred into a glovebox and dried in vacuo before use. NMR spectra were recorded by using *J. Young* valve NMR tubes and obtained on a Bruker AVII+400 (^{1}H: 400.11 MHz, ^{13}C: 100.61 MHz), on a Bruker AVII+500 (^{1}H: 500.13 MHz, ^{13}C: 125.76 MHz, ^{11}B: 160.46 MHz), or on a Bruker DRX 250 (^{1}H: 250.13 MHz, ^{11}B: 80.25 MHz) spectrometer. ^{1}H and ^{13}C shifts are referenced to internal solvent resonances and reported in parts per million relative to TMS. IR spectra were recorded on a NICOLET Impact 410 FTIR spectrometer using a DRIFT chamber with dry KBr/sample mixtures and KBr windows. For the latter the collected data were converted using the Kubelka-Munk refinement. CHN elemental analyses were performed on an Elementar Vario EL III.

Ar = 2,6-diisopropylphenyl throughout the SI.

$Me_2Ga[B(NArCH)_2]$ (2).
To a solution of $(THF)_2Li[B(NArCH)_2]$ (380 mg, 0.706 mmol) in hexane, pre-cooled to –40 °C, was added dropwise a solution of $GaMe_3$ (324 mg, 2.823 mmol) in hexane, pre-cooled to –40 °C. The color disappeared immediately while a white suspension formed. After stirring for 5 min, about 1.5 mL of toluene was added. The mixture was stirred for 40 min at ambient temperature. Afterwards, it was centrifuged and the residue washed 3 times with each 3 mL of hexane. The soluble parts were dried in vacuo for 3 d. The resulting slightly yellow powder still contained THF, therefore a hexane solution of another equivalent of $GaMe_3$ (81 mg, 0.705 mmol) was added to a suspension of the product in about 10 mL of hexane. Toluene (ca. 6 mL) was added until an almost clear solution formed. It was stirred for 50 min at ambient temperature and then dried in vacuo. For separation of the $Me_2Ga[B(NArCH)_2]$, the powder was suspended in 6.5 mL of hexane, centrifuged, and the soluble part dried in vacuo. The completely THF-free-product was obtained in 70% yield (240 mg).

^{1}H NMR (C_6D_6, 400 MHz, 26 °C): $\delta = 7.25$ (2 H, *p*-C_6H_3-*i*Pr_2, m, A part of AB_2 spin system, ^3J = 7.8 Hz), 7.16 (4 H, *m*-C_6H_3-*i*Pr_2, m, B_2 part of AB_2 spin system, ^3J = 7.8 Hz), 6.35 (s, 2 H, NC*H*), 3.19 (sep, 4 H, C*H*Me_2, ^3J = 6.9 Hz), 1.20 (d, 12 H, CH*Me*$_2$), 1.18 (d, 12 H, CH*Me*$_2$), -0.20 (s, 6 H, GaMe_2) ppm.
^{13}C {^{1}H} NMR (C_6D_6, 101 MHz, 26 °C): δ = 146.0 (*o*-C_6H_3-*i*Pr_2), 140.5 (*i*-C_6H_3-*i*Pr_2), 127.9 (*p*-C_6H_3-*i*Pr_2, under peak of C_6H_6), 123.6 (*m*-C_6H_3-*i*Pr_2), 121.1 (N*C*H), 28.7 (*C*HMe_2), 24.7 (CH*Me*$_2$), 3.6 (Ga*Me*$_2$) ppm.
^{11}B {^{1}H} NMR (C_6D_6, 80 MHz, 26 °C): $\delta = 31.3$ ppm.
IR (DRIFT): 3096 (w), 3068 (m), 3026 (w), 2955 (vs), 2920 (s), 2866 (s), 1932 (w), 1864 (w), 1590 (w), 1510 (w), 1468 (s), 1454 (s), 1381 (s), 1356 (m), 1325 (m), 1269 (m), 1255 (m), 1227 (w), 1187 (m), 1180 (m), 1114 (m), 1100 (m), 1058 (m), 932 (m), 906 (w), 803 (m), 758 (s), 704 (s), 634 (m), 555 (s), 534 (m), 447 (w) cm^{-1}.
Elemental analysis (%) calcd for $C_{28}H_{42}BGaN_2$ (487.164 g mol^{-1}): C 69.03; H 8.69; N 5.75. Found: C 69.31; H 8.72; N 5.75.

$(THF)Me_2Ga[B(NArCH)_2]$ (3).
A stock solution of THF in hexane was prepared from 105 mg of THF in 10 mL of hexane. To a solution of $Me_2Ga[B(NArCH)_2]$ (71 mg, 0.146 mmol) in hexane, pre-cooled to –40 °C, was added 1 mL of the stock-solution of THF in hexane, pre-cooled to –40 °C. The mixture was stirred for 135 min at ambient temperature and concentrated in vacuo. Crystals were grown at –40 °C, separated and 2 times shortly dried in vacuo (about 10 min), yielding 27 mg of the clean product (33%).

^{1}H NMR (C_6D_6, 400 MHz, 26 °C): δ = 7.24 (2 H, *p*-C_6H_3-*i*Pr_2, m, A part of AB_2 spin system, ^3J = 8.0 Hz), 7.18 (4 H, *m*-C_6H_3-*i*Pr_2, m, B_2 part of AB_2 spin system, ^3J = 8.0 Hz), 6.38 (s, 2 H, NC*H*), 3.33 (sep, 4 H, C*H*Me_2, ^3J = 7.0 Hz), 3.21 (m, 4 H, THF), 1.27 (d, 12 H, CH*Me*$_2$, ^3J = 6.9 Hz), 1.23 (d, 12 H, CH*Me*$_2$, ^3J = 6.9 Hz), 1.18 (m, 4 H, THF), -0.30 (s, 6 H, Ga*Me*$_2$) ppm.
^{13}C {^{1}H} NMR (C_6D_6, 101 MHz, 26 °C): δ = 146.3 (*o*-C_6H_3-*i*Pr_2), 141.5 (*i*-C_6H_3-*i*Pr_2), 127.5 (*p*-C_6H_3-*i*Pr_2), 123.4 (*m*-C_6H_3-*i*Pr_2), 121.2 (NCH), 68.5 (THF), 28.7 (*C*HMe_2), 25.4 (THF), 25.3 (CH*Me*$_2$), 24.0 (CH*Me*$_2$), -0.2 (Ga*Me*$_2$) ppm.
^{11}B {^{1}H} NMR (C_6D_6, 80 MHz, 26 °C): δ = 32.0 ppm.
IR (DRIFT): 3065 (m), 3021 (w), 2958 (vs), 2862 (s),1504 (w), 1459 (vs), 1377 (vs), 1361 (s), 1328 (m), 1185 (m), 1112 (m), 1056 (m), 1042 (m), 929 (w), 901 (w), 878 (m), 801 (m), 758 (s), 693 (s), 634 (m), 577 (w), 538 (m), 454 (w) cm^{-1}.
Elemental analysis (%) calcd for $C_{32}H_{50}BGaN_2O$ (559.267 g mol^{-1}): C 68.72; H 9.01; N 5.01. Found: C 68.81; H 7.69; N 5.07.

[LiMe$_3$Ga{B(NArCH)$_2$}]$_4$ (4).
To a suspension of pre-dried MeLi (5 mg; 0.21 mmol) in toluene was added dropwise a solution of an equimolar amount of [B(NArCH)$_2$]GaMe$_2$ (100 mg, 0.21 mmol) in toluene. The white suspension was stirred at ambient temperature for 3 h 15 min and then dried in vacuo. Since residual educt [B(NArCH)$_2$]GaMe$_2$ was detected in the ^{1}H NMR spectrum, another 5 mg MeLi was added to a suspension of the crude product in toluene and the mixture was stirred for another 2 h 15 min. Afterwards, the suspension was centrifuged and the white residue (MeLi) washed 3 times with each 2 mL of toluene. The combined filtrate was dried in vacuo to give a yield of 63 mg (60%) of analytically pure product.

^{1}H NMR (C_6D_6, 500 MHz, 26 °C): δ = 7.23 (*p*-C_6H_3-*i*Pr_2, m, A part of AB_2 spin system), 7.12 (*m*-C_6H_3-*i*Pr_2, B_2 part of AB_2 spin system), 6.42 (s, 8 H, NC*H*), 3.49 (sep, 16 H, C*H*Me_2, ^3J = 6.7 Hz), 1,41 (d, 48 H, CH*Me*$_2$, ^3J = 6.5 Hz), 1.26 (d, 48 H, CH*Me*$_2$, ^3J = 6.8 Hz), -1.14 (s, 36 H, Ga*Me*$_3$) ppm.
^{13}C {^{1}H} NMR (C_6D_6, 126 MHz, 26 °C): δ = 147.2 (*o*-C_6H_3-*i*Pr_2), 143.4 (*i*-C_6H_3-*i*Pr_2), 126.6 (p--C_6H_3-*i*Pr_2), 123.3 (*m*-C_6H_3-*i*Pr_2), 120.9 (NCH), 28.7 (*C*HMe_2), 25.6 (CH*Me*$_2$), 23.6 (CH*Me*$_2$), -6.7 (Ga*Me*$_3$) ppm.
^{11}B {^{1}H} NMR (C_6D_6, 160 MHz, 26 °C): δ = 34.3 ppm.
IR (DRIFT): 3065 (w), 2960 (vs), 2923 (s), 2866 (s), 2812 (w), 1578 (w), 1552 (w), 1463 (s), 1372 (vs), 1325 (m), 1267 (w), 1250 (m), 1192 (w), 1154 (w), 1110 (w), 1061 (w), 934 (w), 897 (w), 815 (w), 805 (w), 763 (w), 744 (w), 728 (w), 693 (m), 665 (m), 519 (w), 461 (w) cm^{-1}.
Elemental analysis (%) calcd for $C_{116}H_{180}B_4Ga_4Li_4N_8$ (2036.556 g mol^{-1}): C 68.41; H 8.91; N 5.50. Found: C 67.94; H 8.44; N 4.85.

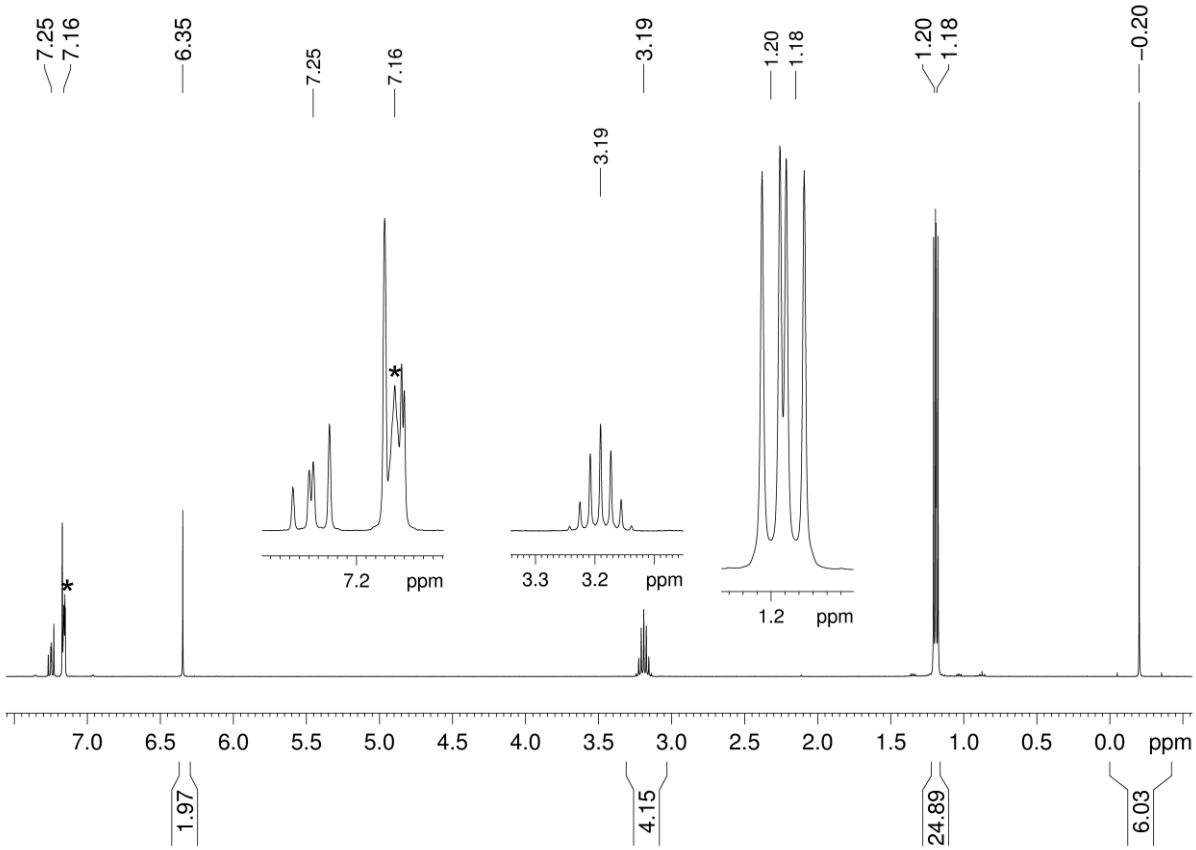

Figure S1. ^{1}H NMR spectrum (400 MHz) of $Me_2Ga[B(NArCH)_2]$ (**2**) in C_6D_6 at 26 °C. The solvent signal is marked by an asterisk.

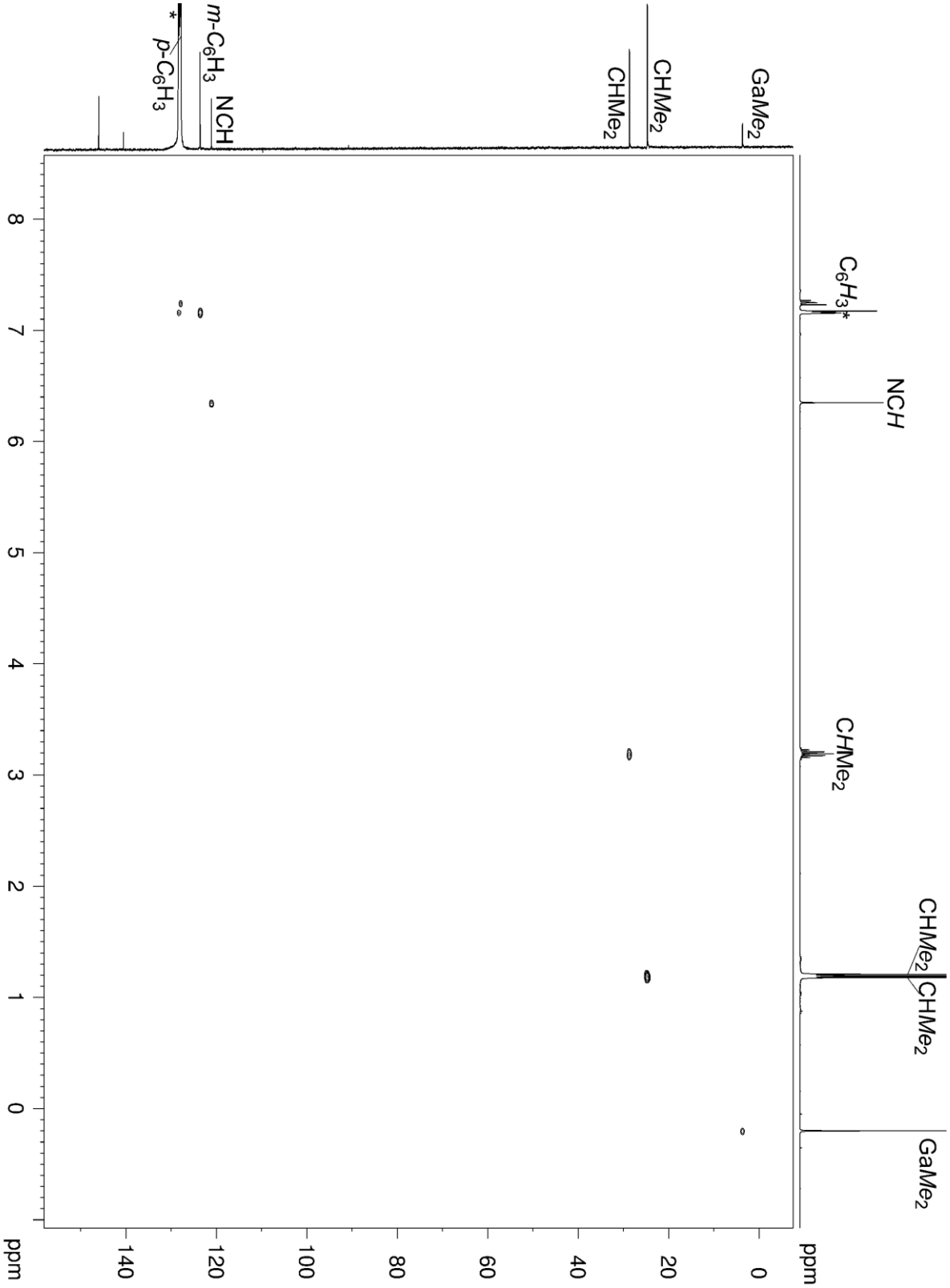

Figure S2. ^{1}H-^{13}C HSQC NMR spectrum (400 MHz/ 101 MHz) of $Me_2Ga[B(NArCH)_2]$ (**2**) in C_6D_6 at 26 °C. The solvent signal is marked by an asterisk.

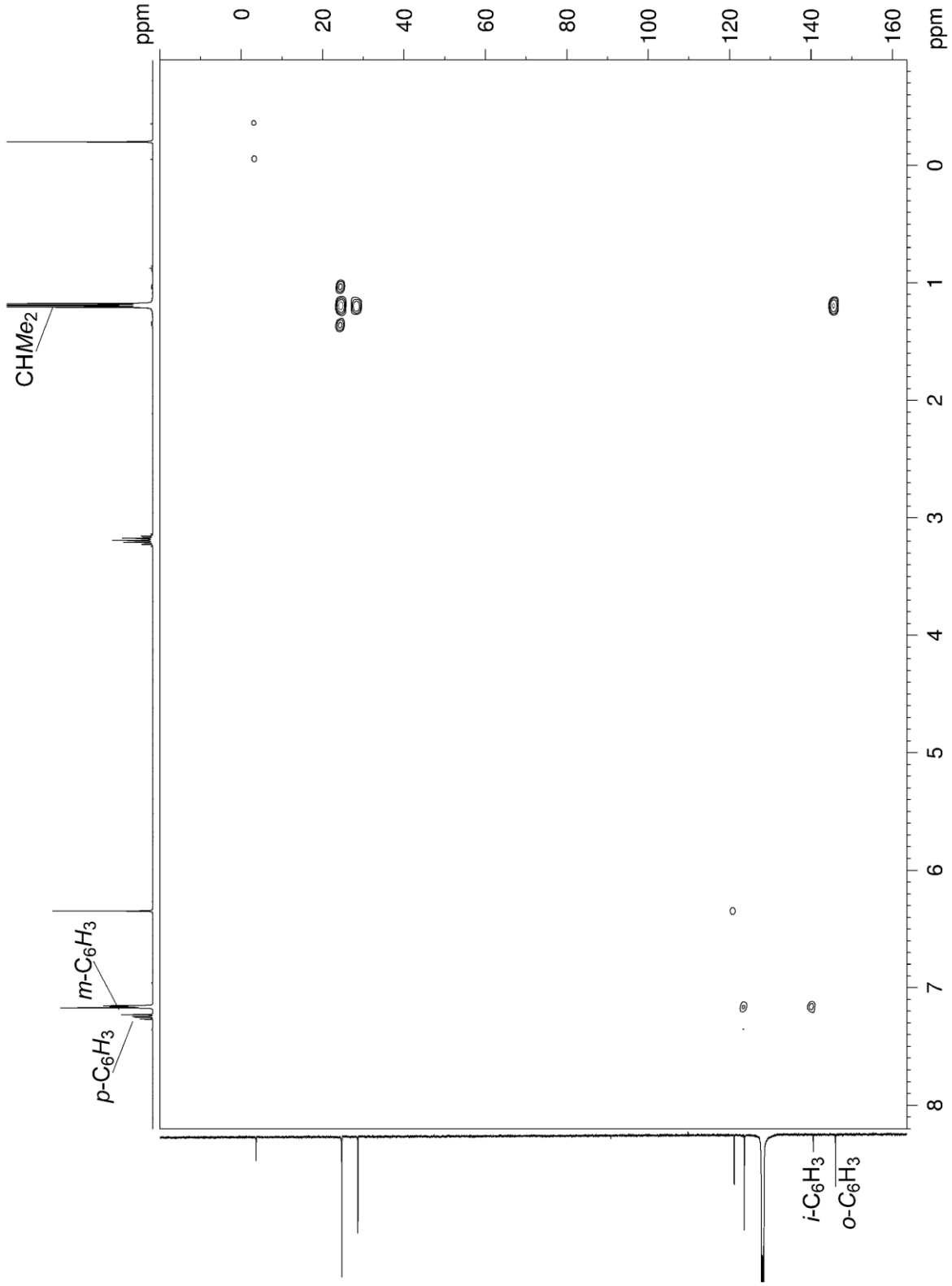

Figure S3. ^{1}H-^{13}C HMBC NMR spectrum (400/101 MHz) of $Me_2Ga[B(NArCH)_2]$ (**2**) in C_6D_6 at 26 °C to assign quaternary C atoms.

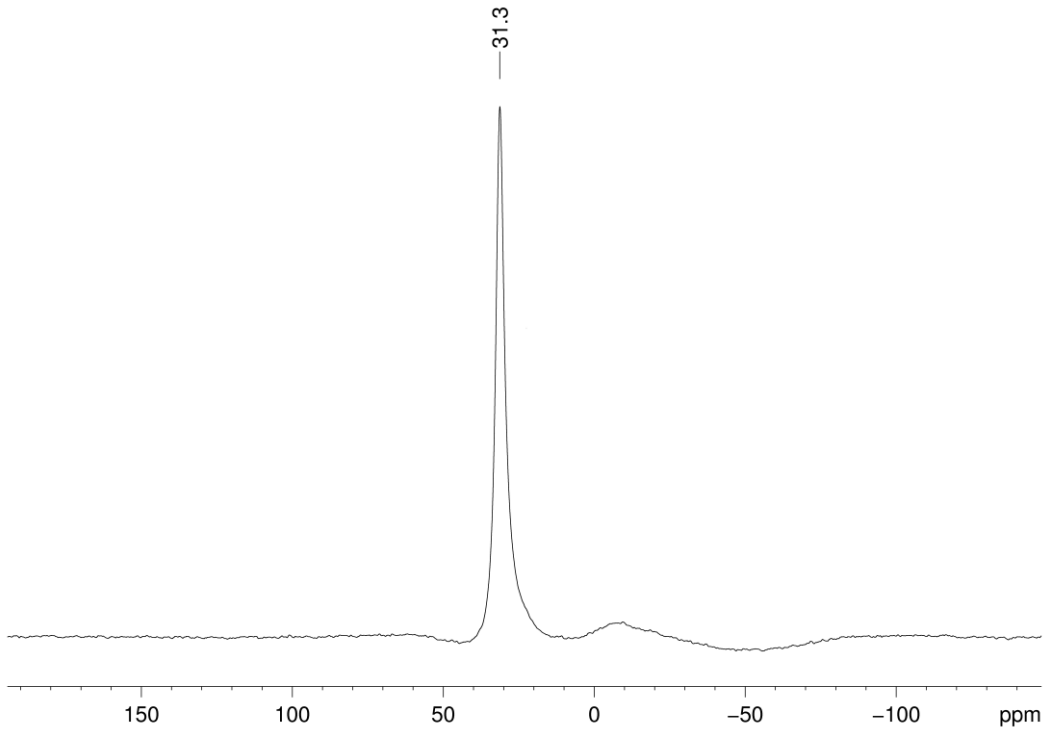

Figure S4. $^{11}B\ \{^{1}H\}$ NMR spectrum (80 MHz) of $Me_2Ga[B(NArCH)_2]$ (**2**) in C_6D_6 at 26 °C.

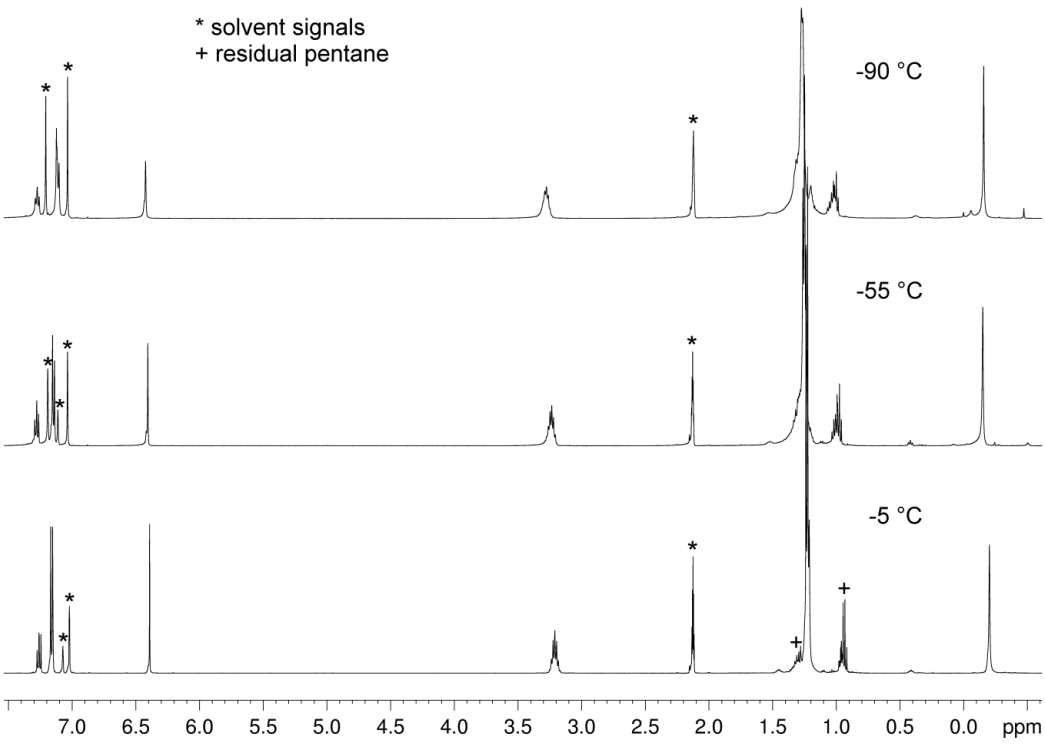

Figure S5. Low-temperature ^{1}H NMR spectra (500 MHz) of $Me_2Ga[B(NArCH)_2]$ (**2**) in toluene-d_8.

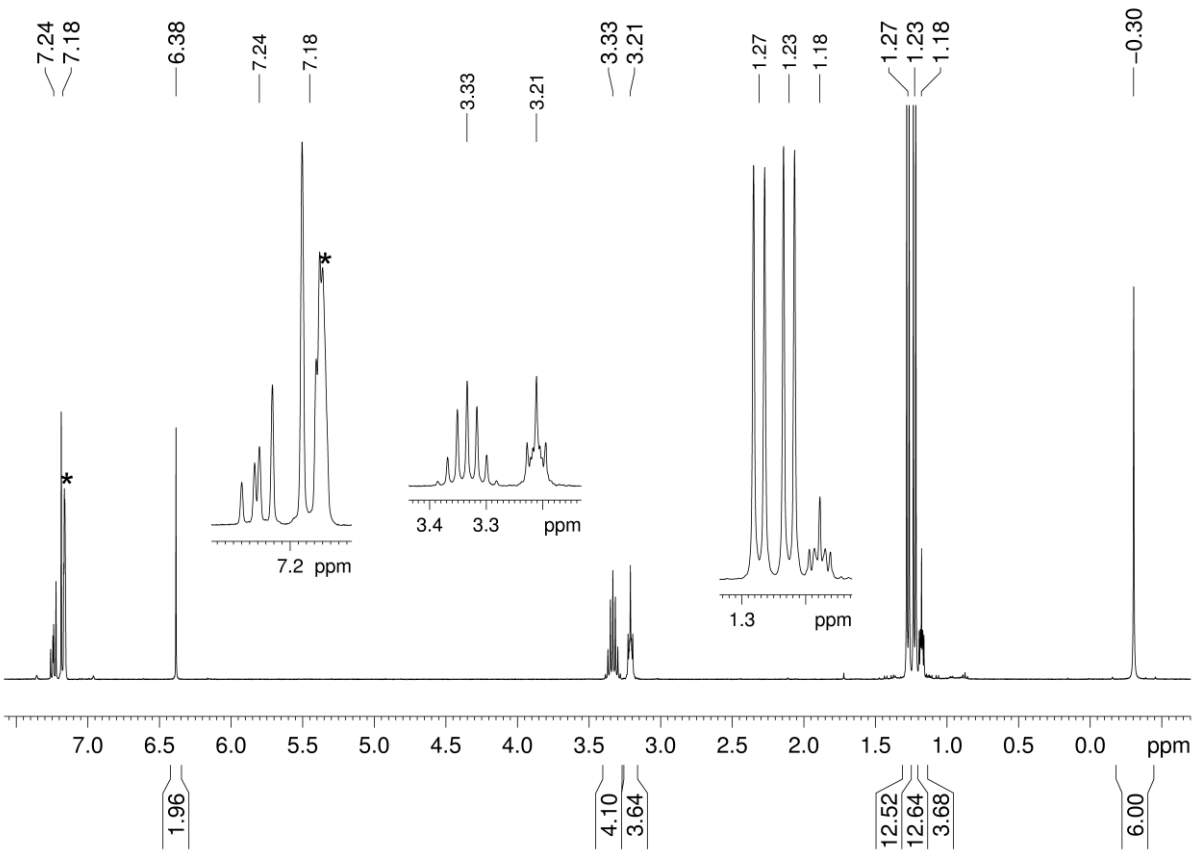

Figure S6. ^{1}H NMR spectrum (400 MHz) of (THF)Me_2Ga[B(NArCH)$_2$] (**3**) in C_6D_6 at 26 °C. The solvent signal is marked by an asterisk.

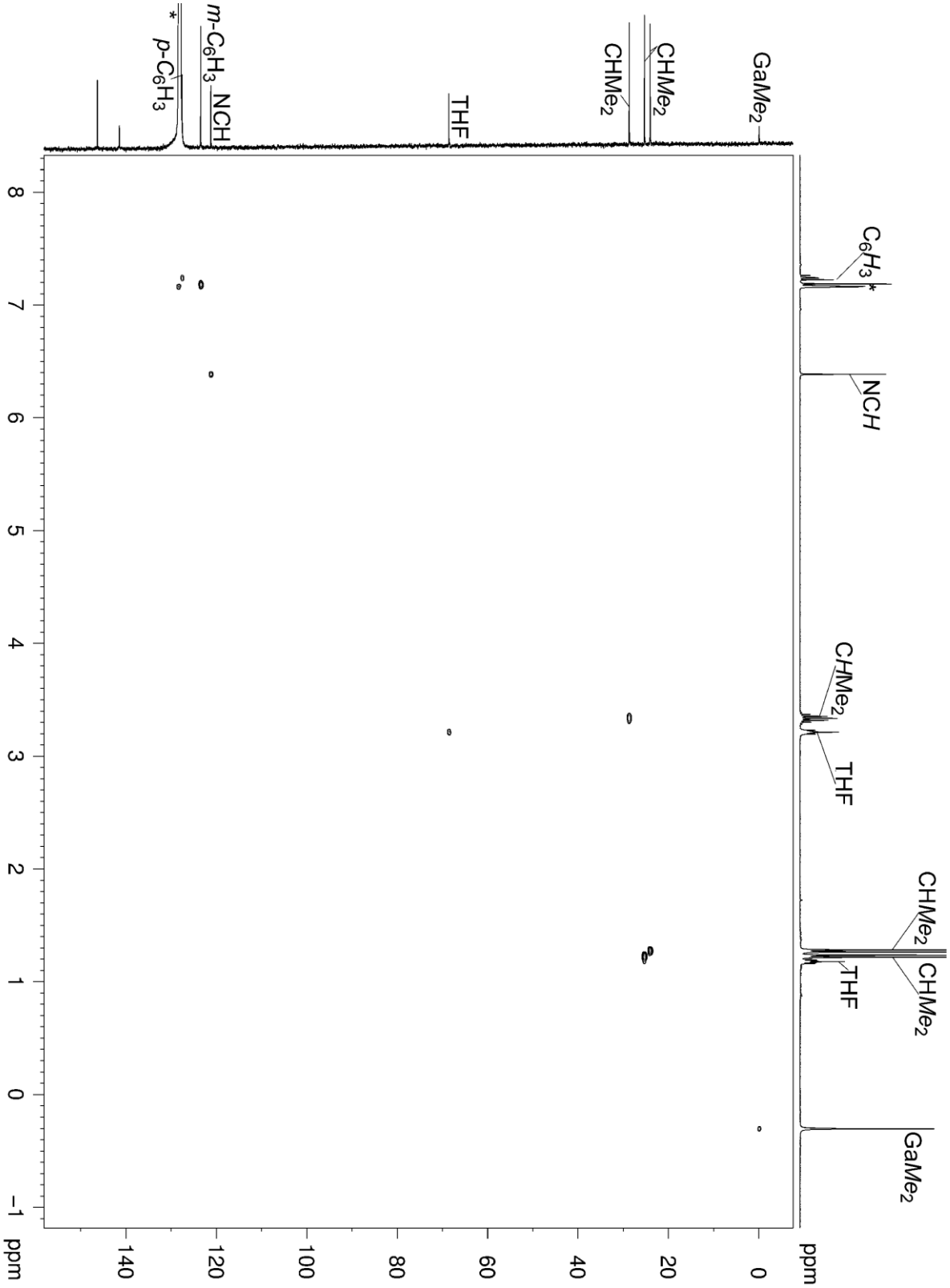

Figure S7. ^{1}H-^{13}C HSQC NMR spectrum (400/ 101 MHz) of (THF)Me_2Ga[B(NArCH)$_2$] (**3**) in C_6D_6 at 26 °C. The solvent signal is marked by an asterisk.

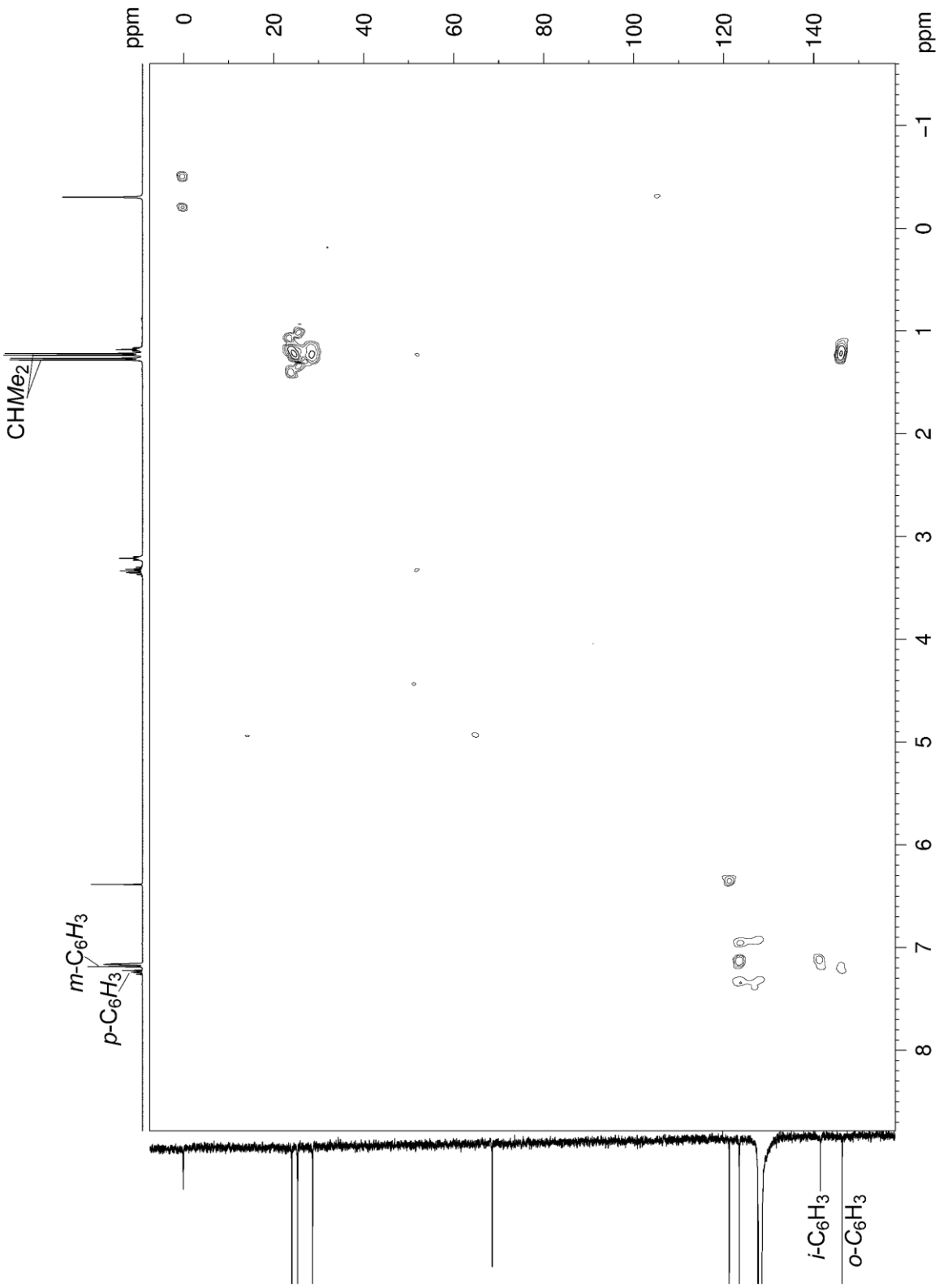

Figure S8. ^{1}H-^{13}C HMBC NMR spectrum (400/101 MHz) of (THF)$Me_2Ga[B(NArCH)_2]$ (**3**) in C_6D_6 at 26 °C to assign quaternary C atoms.

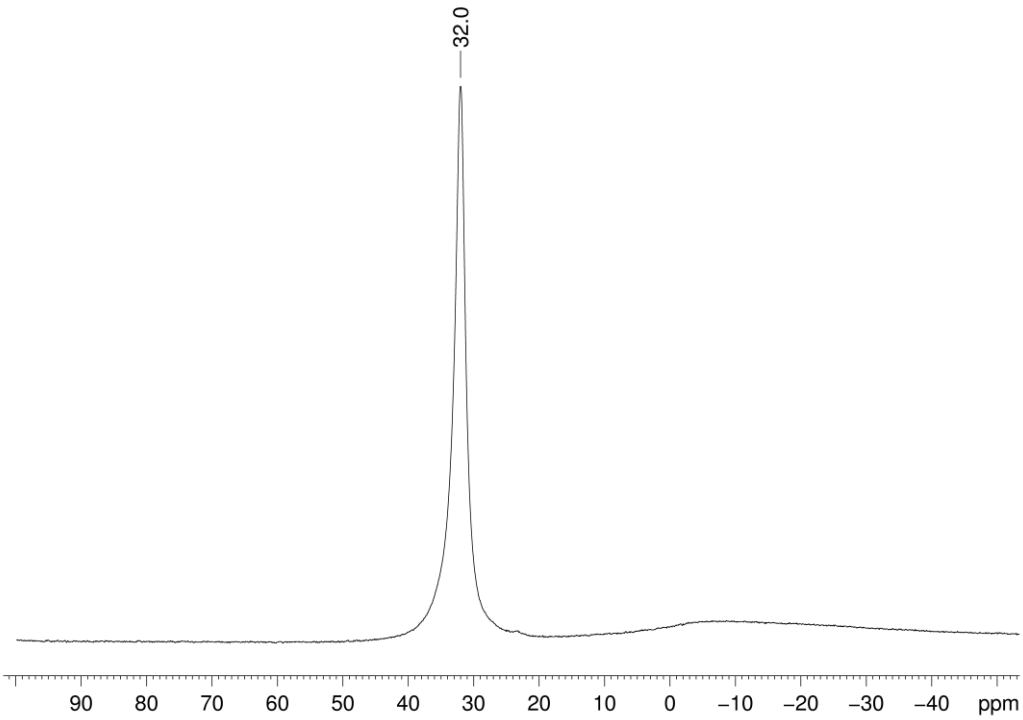

Figure S9. $^{11}B\ \{^{1}H\}$ NMR spectrum (160 MHz) of (THF)$Me_2Ga[B(NArCH)_2]$ (**3**) in C_6D_6 at 26 °C.

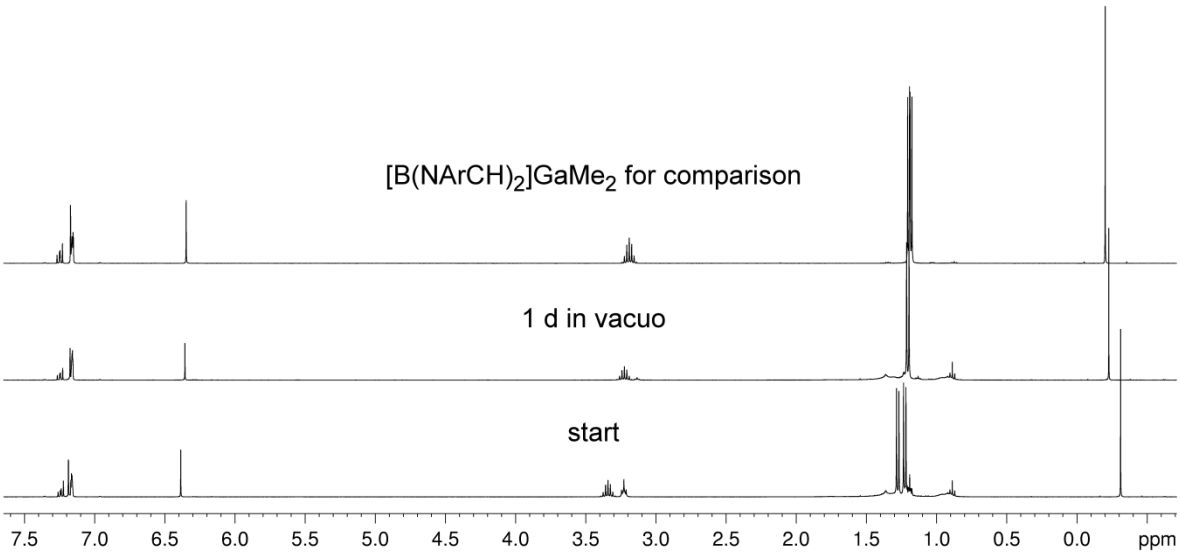

Figure S10. ^{1}H NMR spectra (400 MHz) of (THF)$Me_2Ga[B(NArCH)_2]$ (**3**) in C_6D_6 at 26 °C showing the loss of coordinated THF in vacuo.

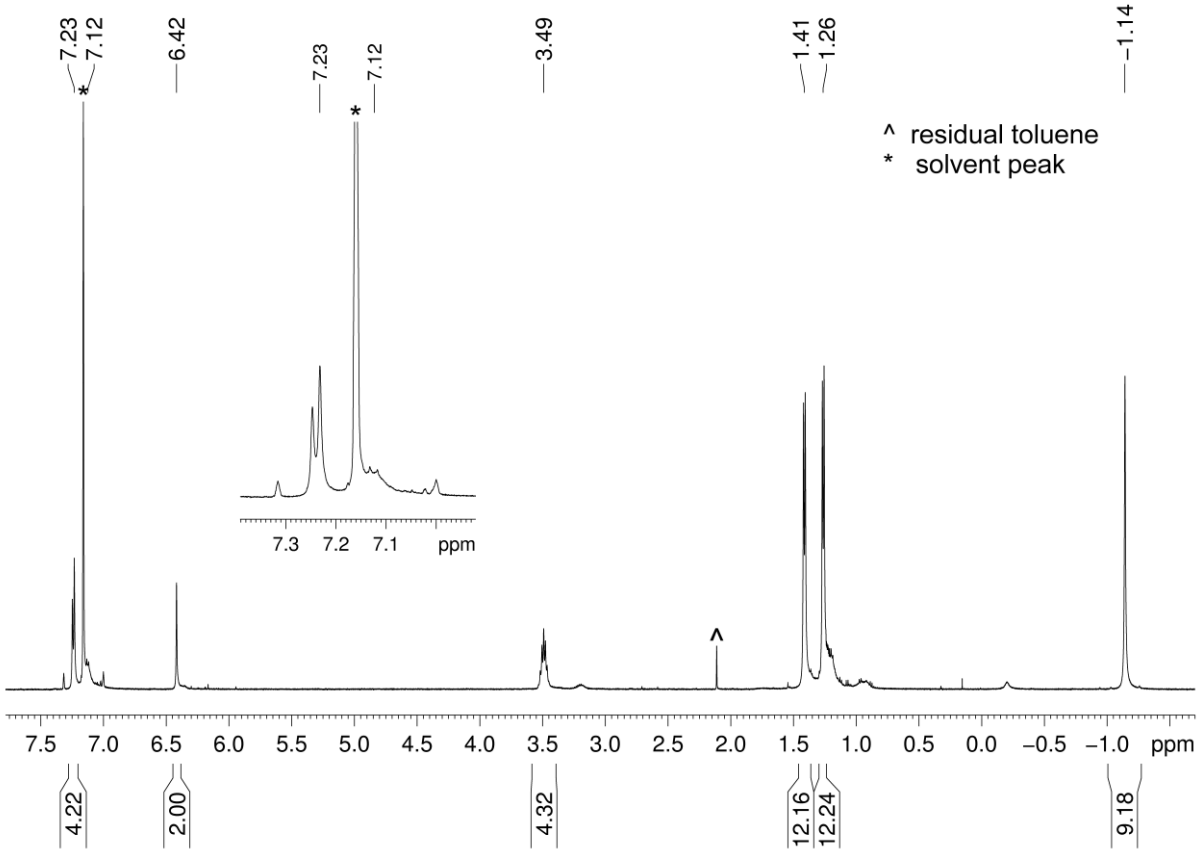

Figure S11. ^{1}H NMR spectrum (500 MHz) of $[LiMe_3Ga\{B(NArCH)_2\}]_4$ (**4**) at 26 °C in C_6D_6.

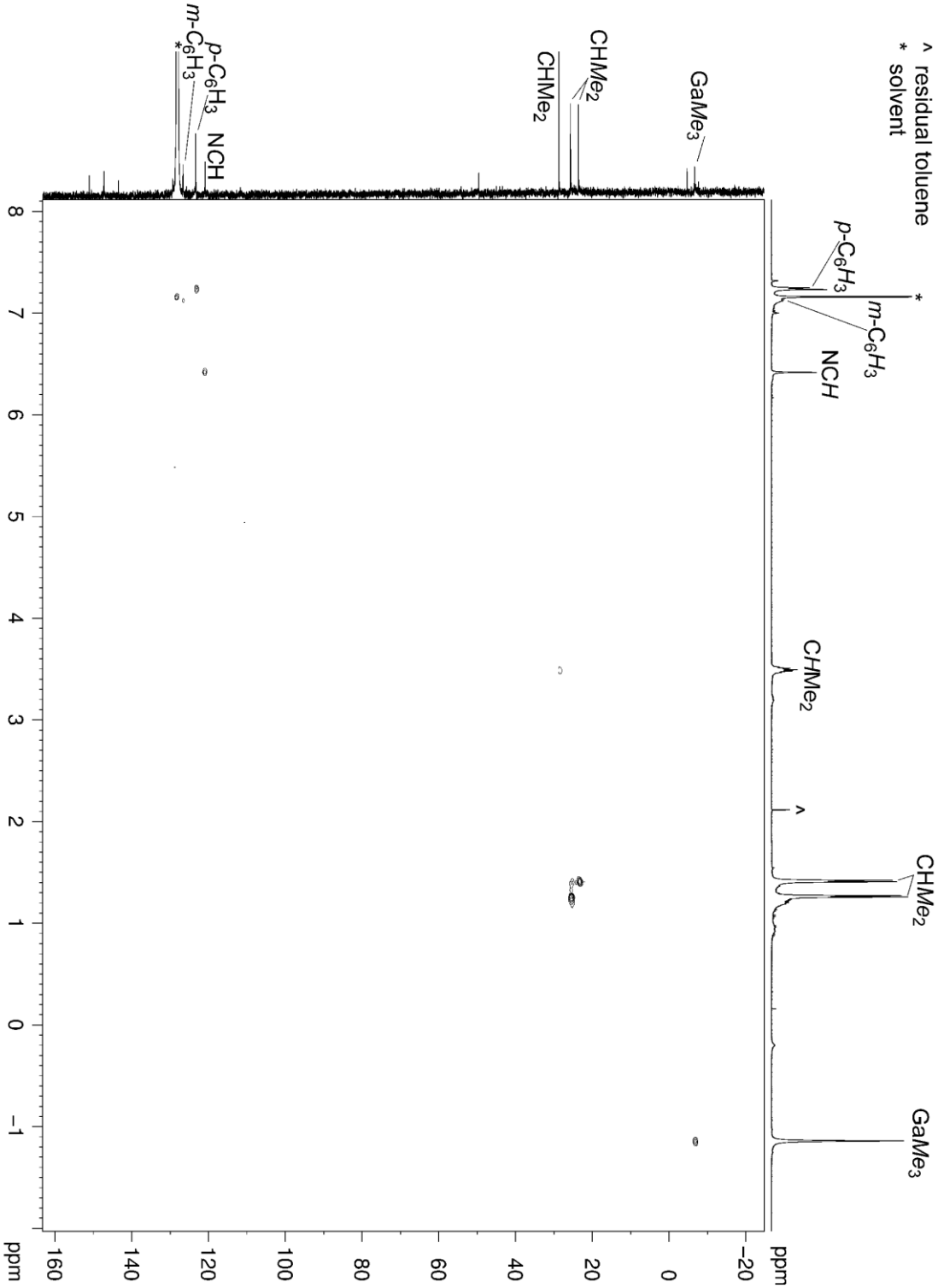

Figure S12. ^{1}H-^{13}C HSQC NMR spectrum (500/ 126 MHz) of $[LiMe_3Ga\{B(NArCH)_2\}]_4$ (**4**) in C_6D_6 at 26 °C.

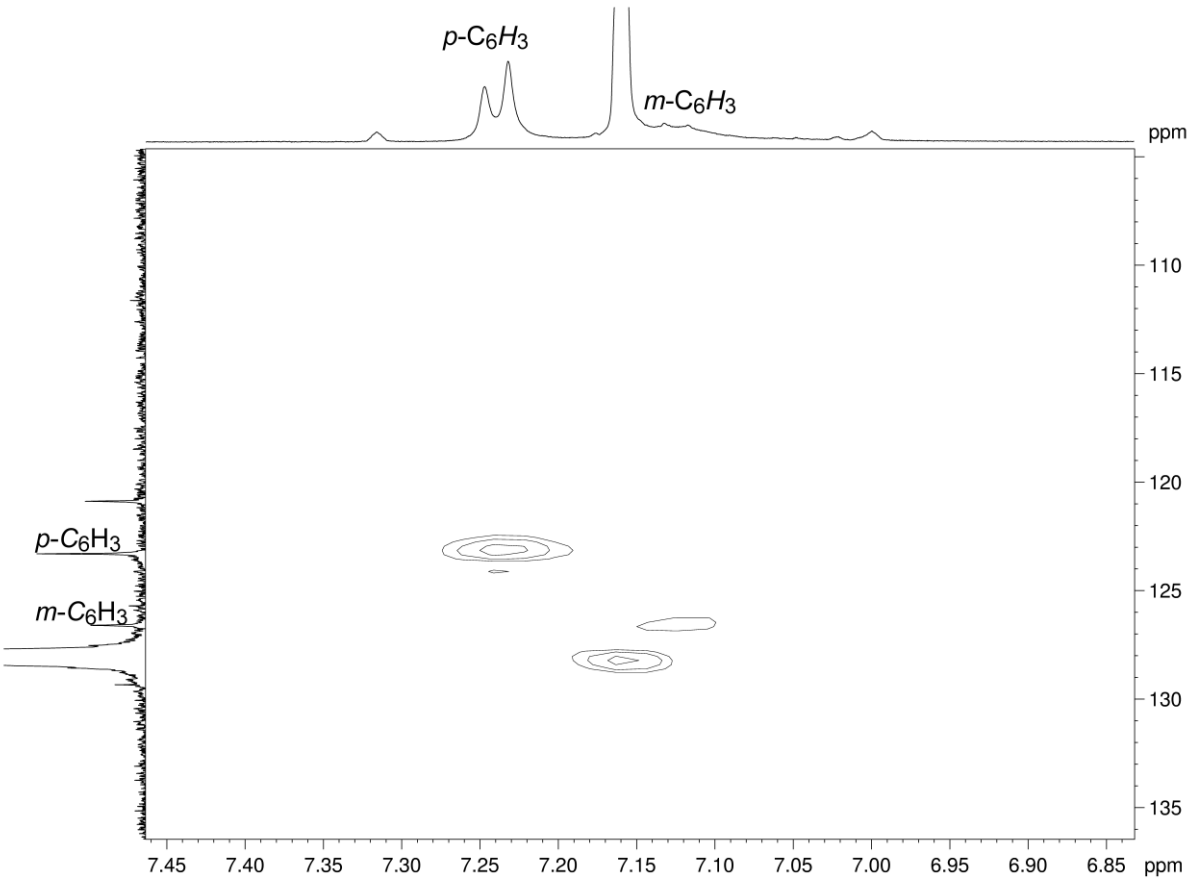

Figure S13. Excerpt of the ^{1}H-^{13}C HSQC NMR spectrum (500/ 126 MHz) of $[LiMe_3Ga\{B(NArCH)_2\}]_4$ (**4**) in C_6D_6 at 26 °C.

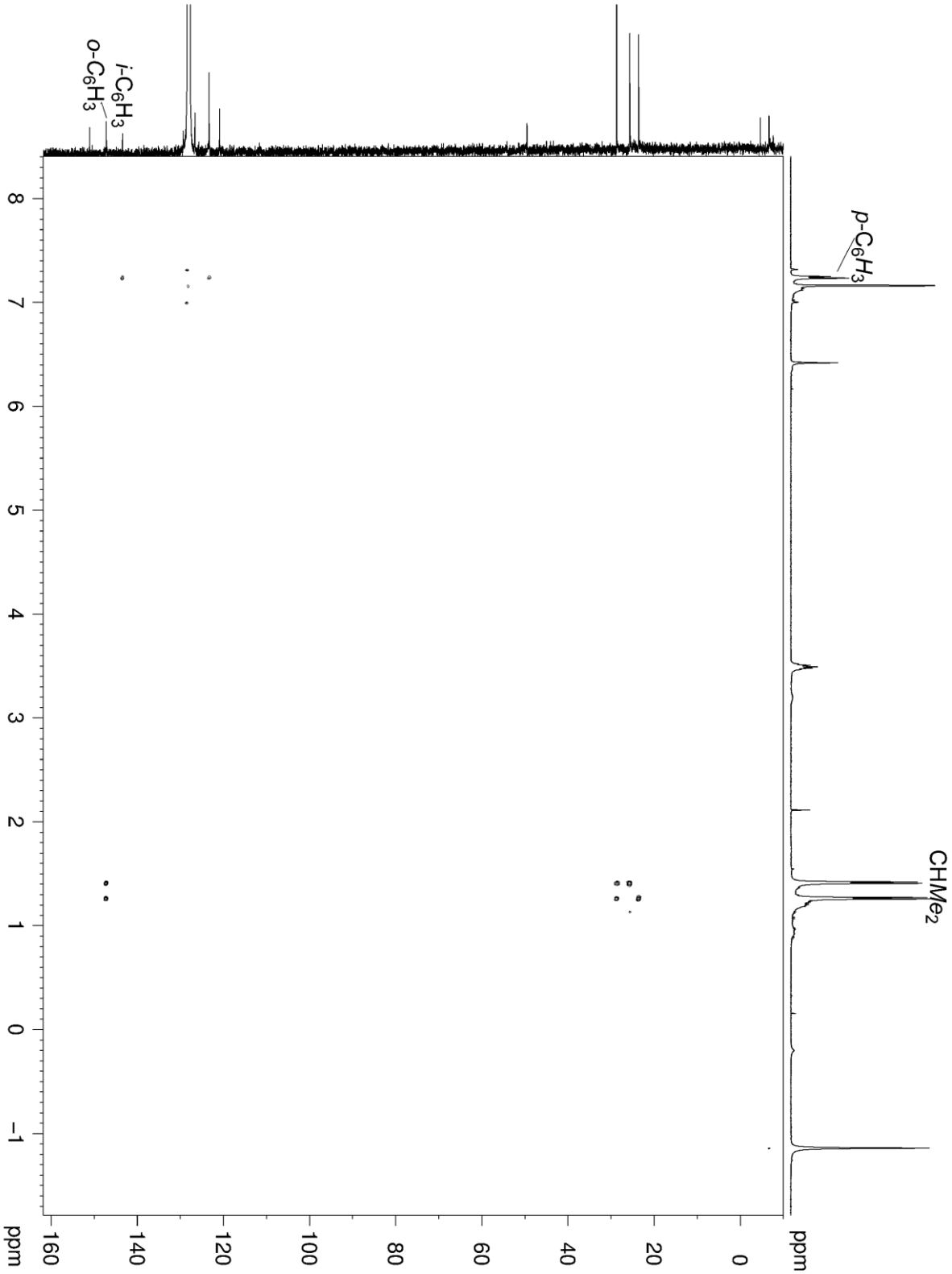

Figure S14. ^{1}H-^{13}C HMBC NMR spectrum (500/126 MHz) of $[LiMe_3Ga\{B(NArCH)_2\}]_4$ (**4**) in C_6D_6 at 26 °C to assign quaternary C atoms.

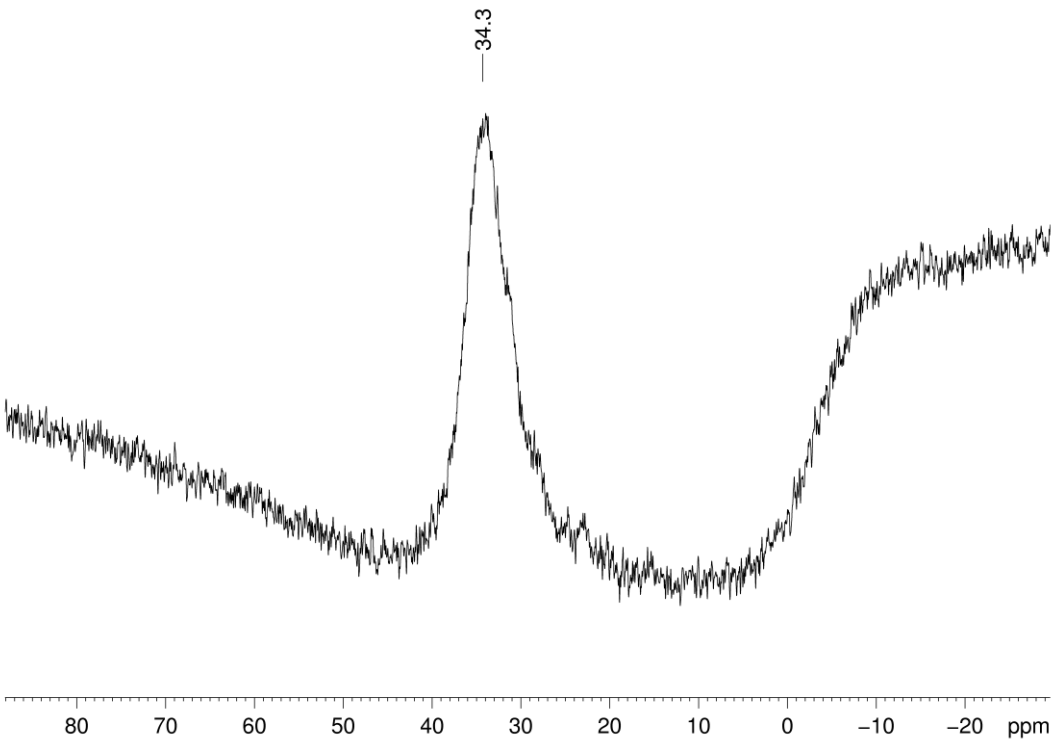

Figure S15. $^{11}B\ \{^{1}H\}$ NMR spectrum (160 MHz) of $[LiMe_3Ga\{B(NArCH)_2\}]_4$ (**4**) in C_6D_6 at 26 °C.

X-ray Crystallographic Investigations

Table S1. Crystallographic Data for Compounds **2**-**4**

	2	**3**	**4**
Formula	$C_{28}H_{42}BGaN_2$	$C_{32}H_{50}BGaN_2O$	$C_{134}H_{198}B_4Ga_4Li_4N_8$
Fw	587.18	559.27	2270.87
temp (K)	173(2)	100(2)	100(2)
cryst syst	orthorhombic	monoclinic	monoclinic
space group	Pcab	P21/c	P 21/c
a (Å)	14.7354(5)	12.1653(9)	19.5718(10)
b (Å)	18.7239(6)	10.6931(8)	18.8267(11)
c (Å)	20.3319(8)	25.5308(19)	20.2279(10)
α (deg)	90	90	90
β (deg)	90	107.966(4)	116.763(2)
γ (deg)	90	90	90
vol (Å^3)	5609.7(3)	3159.2(4)	6655.0(6)
Z	8	4	2
ρ_{calcd} (mg/mm^3)	1.154	1.176	1.133
μ (mm^{-1})	0.997	0.896	0.849
R1^a ($I > 2.0\sigma(I)$)	0.0475	0.0255	0.0420
wR2^b (all data)	0.1031	0.0690	0.0878
diffractometer system	Stoe IPDS2T	SMART APEX II	APEX II DUO
solvent	pentane	hexane	benzene

[a] $R1 = \Sigma(||F_0|-|F_c||)/\Sigma|F_0|$. [b] $wR2 = \{\Sigma[w(F_0^2-F_c^2)^2/\Sigma[w(F_0^2)^2]\}^{1/2}$.

Crystals of **2**, **3** and **4** were grown by standard techniques from saturated solutions at –40 °C. Suitable crystals for X-ray structure analyses were selected in a glovebox and coated with

Paratone-N (Hampton Research). For compound **3**, a drop of toluene was mixed into paratone and pre-cooled at –40 °C before crystal selection. During the transport to the diffractometer, the paratone-coated crystals were cooled at –78 °C.

X-ray data for compound **2** were collected on a STOE IPDS II system using MoK_α radiation (λ = 0.71073 Å) and corrected for Lorentz and polarization effects and absorption by air. Data for **2** was processed using Stoe's X-Area software suite.[1] Data for **3** were collected on a Bruker SMART APEX II instrument by using a TRIUMPH monochromator and MoK_α radiation (λ = 0.71073 Å), with ω and ϕ scans.

Data for **4** were collected on a Bruker APEX DUO instrument by using QUAZAR optics and MoK_α radiation (λ = 0.71073 Å), with ω and ϕ scans. The raw data were processed by using APEX2[2] and SAINT softwares;[3] structure solution and final model refinement were performed by using SHELXTL.[4] Corrections for absorption effects were applied by using SADABS.[5] All graphics were produced by using ORTEP-3[6] and POV-Ray.[7] CCDC-949222 (**2**), CCDC-949223 (**3**), and CCDC-972035 (**4**) contain the supplementary crystallographic data for this paper. These data can be obtained free of charge from The Cambridge Crystallographic Data Centre via www.ccdc.cam.ac.uk/data_request/cif.

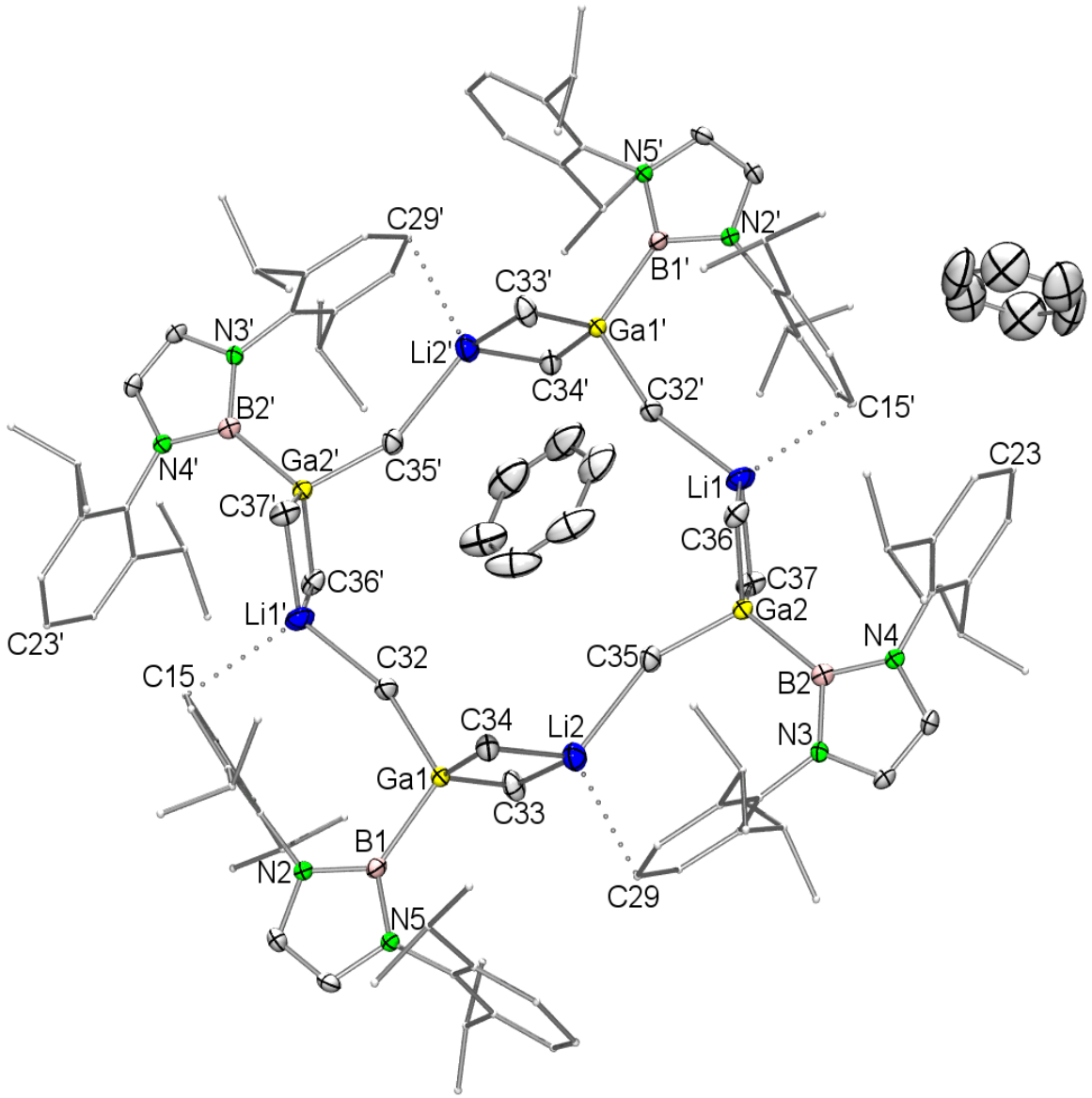

Figure S16. Molecular structure of **4** with atomic displacement parameters set at the 50% level. Co-crystallized benzene-d_6 molecules are shown. Hydrogen atoms are omitted and the aromatic parts are shown with reduced radius for clarity.

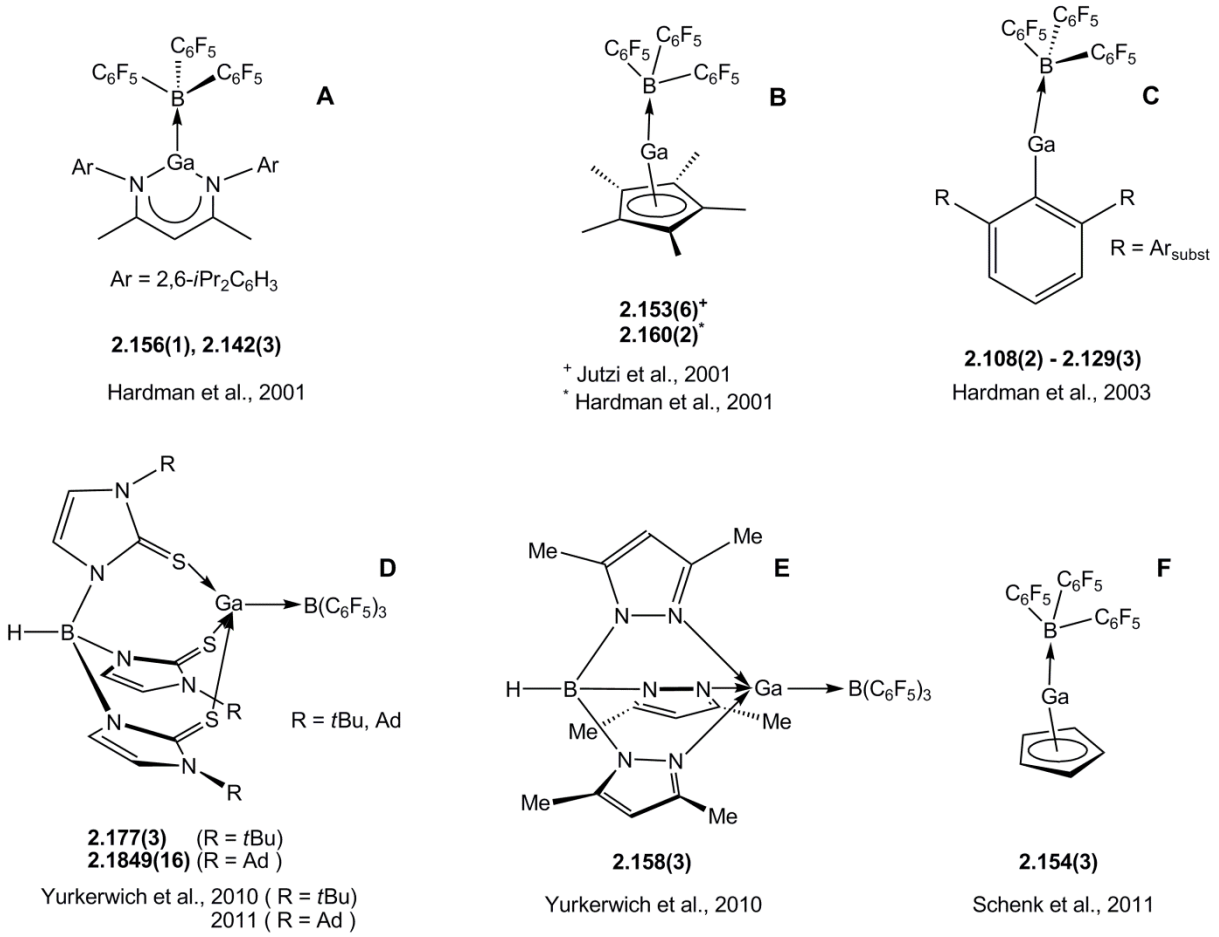

Chart S1. Complexes with B−Ga bonds (bond lengths in Å). **A**: two indpendent molecules in the solid state; **B**: two times crystallographically characterized,* ref. 8, + ref. 9.

Computational details

DFT calculations of all the systems reported were performed with the GAUSSIAN 09 program suite[10] using the B3LYP density functional,[11] along with the implemented 6-311G(d,p) basis set.[12] All geometry optimizations were initially carried out without imposing any symmetry constraints. The geometries of **1a** and **2a**, however, converged close to C_{2v} symmetry and were subsequently optimized within this symmetry. All geometrical parameters were in good agreement with their experimental counterparts, the only exception being a larger deviation for the relative orientation of the aryl substituents in **2a**: In the X-ray structure of **2,** the dihedral angle between the aryl substituent and the molecular plane averages 73.1°, whereas in **2a** it increases to 89.5° (see Fig. S17), which is most likely due to the absence of crystal-packing effects in the DFT model. This almost perpendicular orientation is accompanied by a nearly symmetric alignment of the *iso*-propyl groups. All structures were confirmed as true minima on the respective potential energy surface by calculating analytical frequencies. Only in the case of the free boryl anion, **1a**, one spurious imaginary frequency of $\omega = i8.7$ cm^{-1} was found. The topology of the electron density was analyzed using the software package AIMALL;[13] the computation of natural bond orbitals (NBOs) for **2a** was performed using the algorithm in version 3.1 of the NBO program,[14] as implemented in GAUSSIAN 09.[10] Plots were generated using AIMALL[13] and CHEMCRAFT.[15]

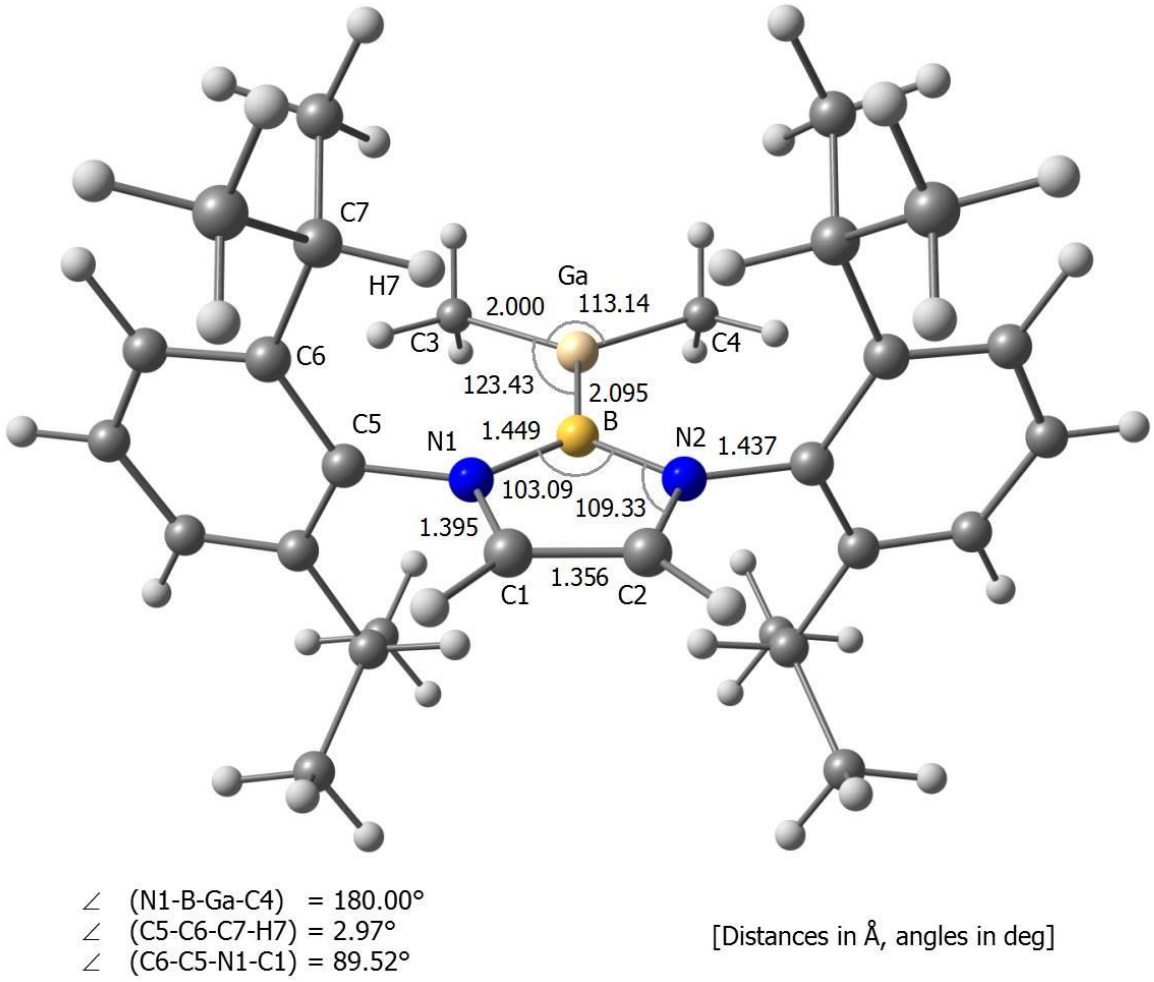

Figure S17. Optimized geometry (C_{2v} symmetry) and selected geometrical parameters for $[Me_2Ga\{B(NArCH)_2\}]$ (**2a**) (Ar = C_6H_3-2,6-*i*Pr_2).

Cartesian Coordinates for **2a**:

6	-3.335716000	3.031484000	-1.837940000
6	-3.335716000	-3.031484000	-1.837940000
6	0.000000000	-0.677814000	-2.184435000
6	-2.570812000	2.513408000	-0.605283000
6	0.000000000	0.677814000	-2.184435000
6	-2.570812000	-2.513408000	-0.605283000
6	-3.433773000	2.622790000	0.665150000
6	-1.229123000	3.220133000	-0.444073000
6	-1.201587000	4.590134000	-0.166763000
6	-1.229123000	-3.220133000	-0.444073000
6	3.335716000	-3.031484000	-1.837940000
6	-1.201587000	-4.590134000	-0.166763000
6	0.000000000	-2.541989000	-0.574278000
6	0.000000000	2.541989000	-0.574278000
6	-3.433773000	-2.622790000	0.665150000
6	3.335716000	3.031484000	-1.837940000
6	0.000000000	5.272173000	-0.026880000
6	0.000000000	-5.272173000	-0.026880000

6	1.229123000	-3.220133000	-0.444073000
6	1.201587000	-4.590134000	-0.166763000
6	2.570812000	-2.513408000	-0.605283000
6	1.229123000	3.220133000	-0.444073000
6	1.201587000	4.590134000	-0.166763000
6	2.570812000	2.513408000	-0.605283000
6	3.433773000	-2.622790000	0.665150000
6	3.433773000	2.622790000	0.665150000
6	0.000000000	-1.669051000	3.232020000
6	0.000000000	1.669051000	3.232020000
1	-4.270115000	2.477439000	-1.968719000
1	-2.743461000	2.915167000	-2.749026000
1	-2.743461000	-2.915167000	-2.749026000
1	-4.270115000	-2.477439000	-1.968719000
1	-3.587788000	4.091233000	-1.736670000
1	0.000000000	-1.357132000	-3.021882000
1	0.000000000	1.357132000	-3.021882000
1	-3.587788000	-4.091233000	-1.736670000
1	-2.367565000	1.454331000	-0.770256000
1	-2.367565000	-1.454331000	-0.770256000
1	-4.357624000	2.048345000	0.548448000
1	2.743461000	-2.915167000	-2.749026000
1	-2.135353000	5.130711000	-0.059317000
1	2.743461000	2.915167000	-2.749026000
1	-4.357624000	-2.048345000	0.548448000
1	-2.135353000	-5.130711000	-0.059317000
1	-3.713517000	3.659120000	0.875363000
1	3.587788000	-4.091233000	-1.736670000
1	4.270115000	-2.477439000	-1.968719000
1	3.587788000	4.091233000	-1.736670000
1	-2.901882000	2.239822000	1.539429000
1	-3.713517000	-3.659120000	0.875363000
1	0.000000000	6.334884000	0.189417000
1	0.000000000	-6.334884000	0.189417000
1	2.367565000	-1.454331000	-0.770256000
1	4.270115000	2.477439000	-1.968719000
1	-2.901882000	-2.239822000	1.539429000
1	2.135353000	-5.130711000	-0.059317000
1	2.135353000	5.130711000	-0.059317000
1	2.367565000	1.454331000	-0.770256000
1	4.357624000	-2.048345000	0.548448000
1	3.713517000	-3.659120000	0.875363000
1	3.713517000	3.659120000	0.875363000
1	2.901882000	-2.239822000	1.539429000
1	0.000000000	2.586871000	2.641962000
1	4.357624000	2.048345000	0.548448000
1	0.000000000	-2.586871000	2.641962000
1	2.901882000	2.239822000	1.539429000
1	-0.877017000	-1.681472000	3.889109000
1	0.877017000	1.681472000	3.889109000
1	-0.877017000	1.681472000	3.889109000
1	0.877017000	-1.681472000	3.889109000
5	0.000000000	0.000000000	0.035199000
31	0.000000000	0.000000000	2.130140000
7	0.000000000	-1.135020000	-0.866145000
7	0.000000000	1.135020000	-0.866145000

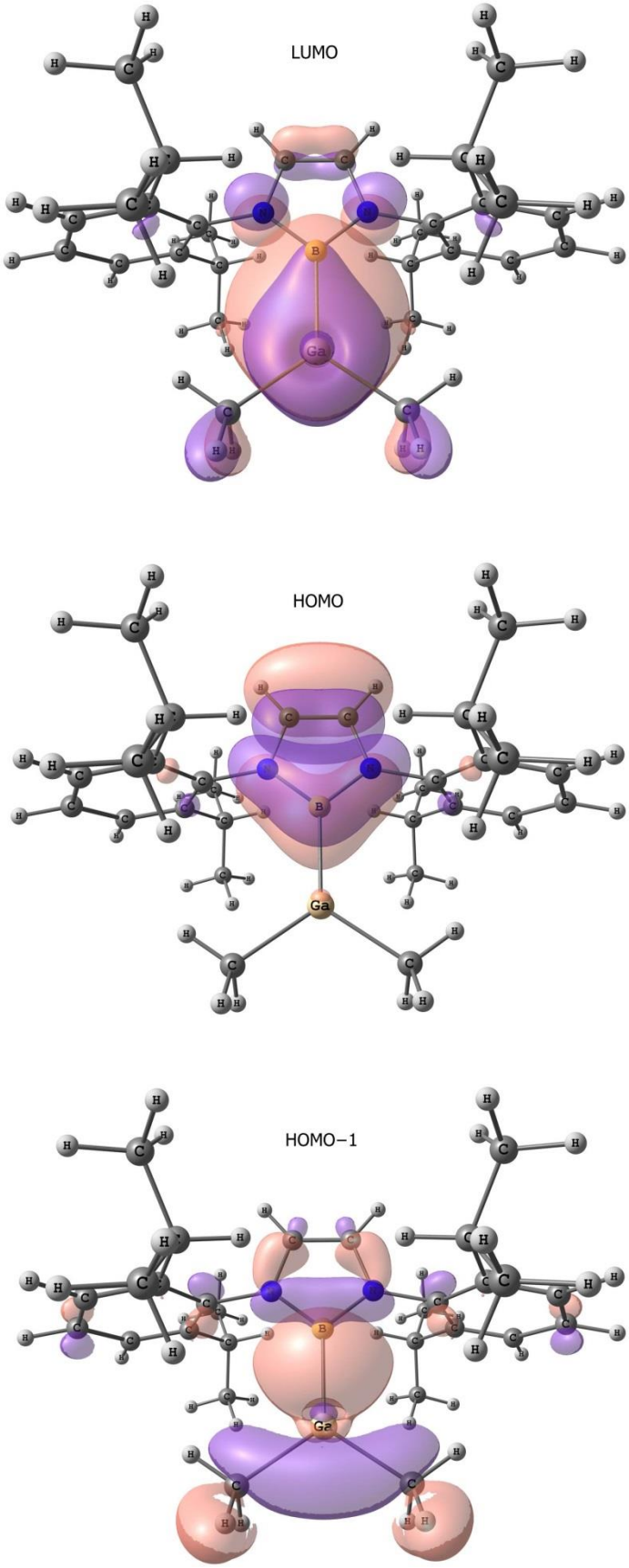

Figure S18. 3D representation of selected molecular orbitals of [$Me_2Ga\{B(NArCH)_2\}$] (**2a**) (Ar = C_6H_3-2,6-*i*Pr_2).

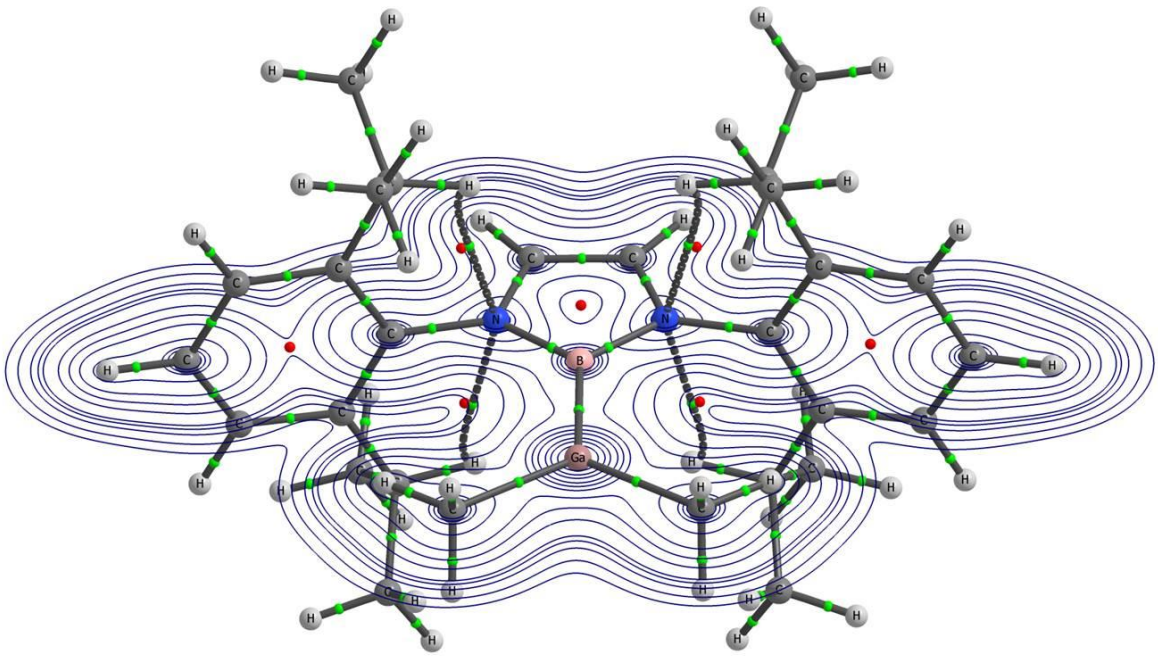

Figure S19. Contour plot of the electron density, $\rho(\mathbf{r})$, in the molecular plane of $[Me_2Ga\{B(NArCH)_2\}]$ (**2a**) (Ar = C_6H_3-2,6-*i*Pr_2), with bond paths superimposed; BCPs and RCPs are represented by green and red points, respectively. Dashed bond paths indicate weak C−H···N interactions; other BCPs with ρ_b < 0.01 e bohr^{-3} (C−H···C interactions) are not shown.

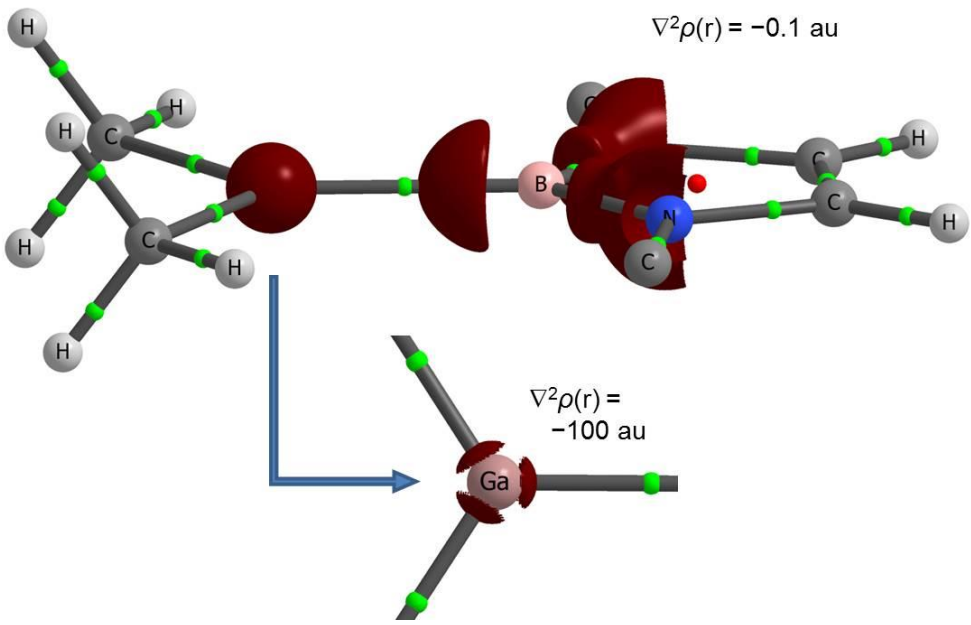

Figure S20. Isosurface plots of the negative Laplacian of **2a** in the vicinity of B and Ga at $\nabla^2\rho(\mathbf{r})$ = −0.1 au (top) and $\nabla^2\rho(\mathbf{r})$ = −100 au (bottom, view from above the molecular plane). The charge concentrations around Ga are visible only at high negative values of $\nabla^2\rho(\mathbf{r})$: The three maxima, i.e. (3,+3) critical points of $\nabla^2\rho(\mathbf{r})$, occur at ca. −109 au, while (3,−1) critical points of $\nabla^2\rho(\mathbf{r})$ (local charge minima in two dimensions) are observed at values of $\nabla^2\rho(\mathbf{r})$ between −95.3 and −98.9 au.

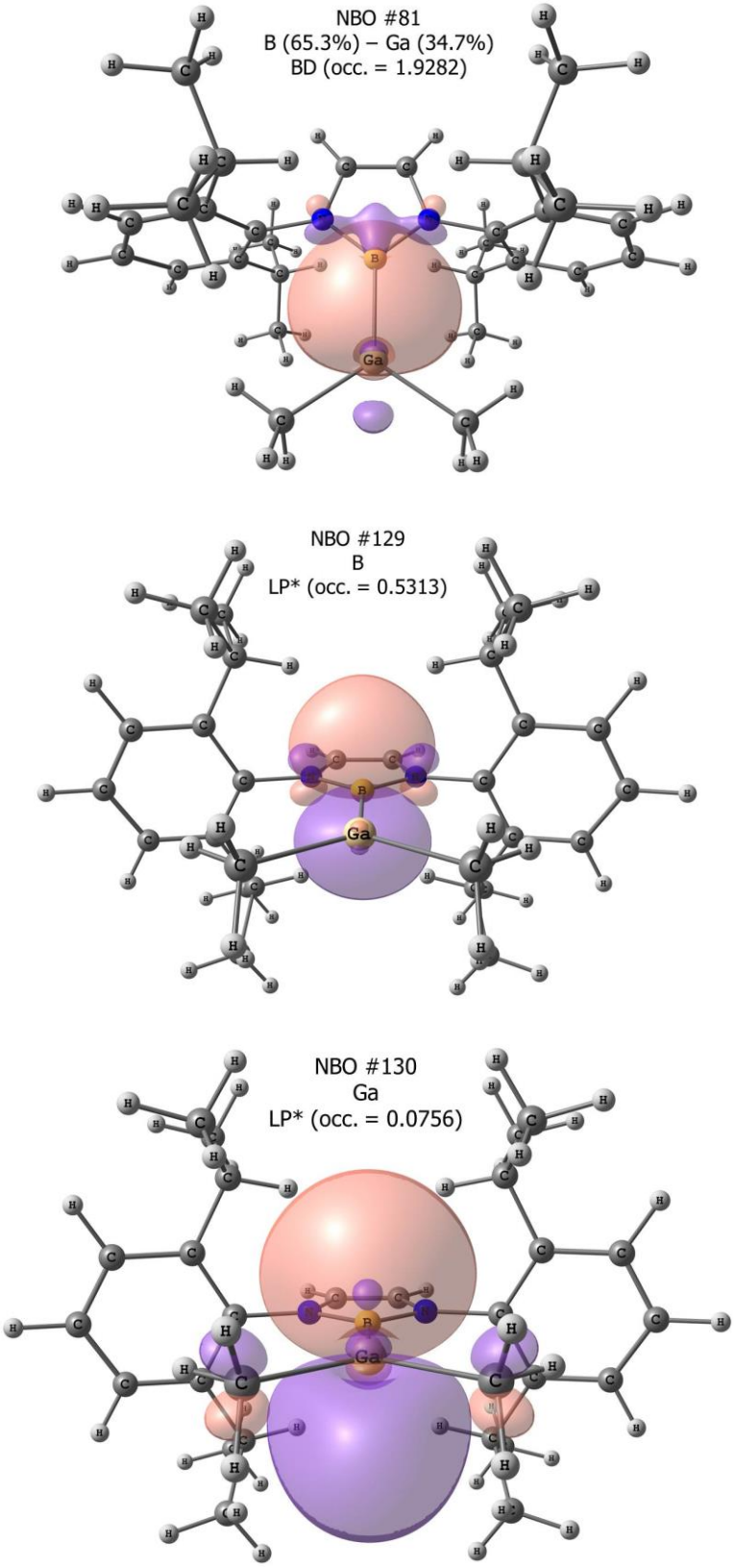

Figure S21. 3D representation of selected natural bond orbitals of [$Me_2Ga\{B(NArCH)_2\}$] (**2a**) (Ar = C_6H_3-2,6-*i*Pr_2). For the latter two, a donor-acceptor interaction is proposed according to the NBO scheme.

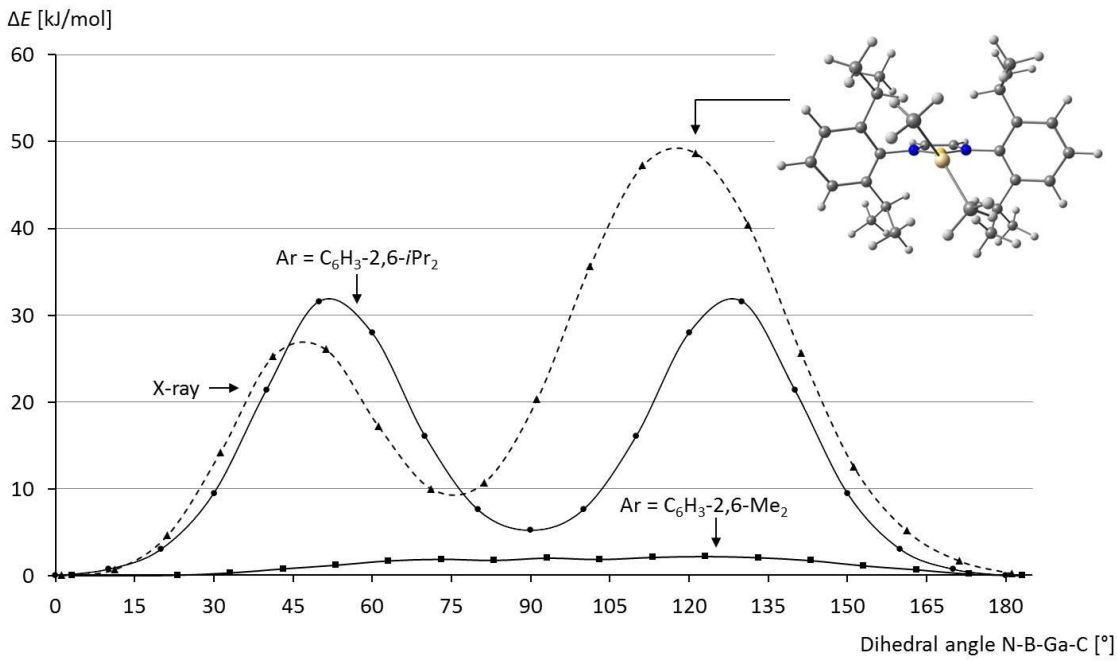

Figure S22. Rigid potential energy surface (PES) scan for the DFT-optimized model systems [$Me_2Ga\{B(NArCH)_2\}$], with two different aryl substituents (Ar = C_6H_3-2,6-*i*Pr_2, **2a**, C_{2v} symmetry; and Ar = C_6H_3-2,6-Me_2, C_2 symmetry), showing the dependence of the total energy on the dihedral angle N-B-Ga-C. The plot clearly indicates that the higher energies observed for intermediate angles in **2** are due to steric crowding. Replacement of the *i*-propyl substituents in **2a** by methyl groups removes the steric strain at intermediate angles, and the PES scan for this model system (Ar = C_6H_3-2,6-Me_2) shows that the total energy does not change significantly with the dihedral angle. This demonstrates that there are no significant π interactions between B and Ga. A PES scan for **2a,** starting from the X-ray geometry, is also included and indicated by a dashed line; this PES curve is asymmetric, as the experimental geometry deviates from C_{2v} symmetry.

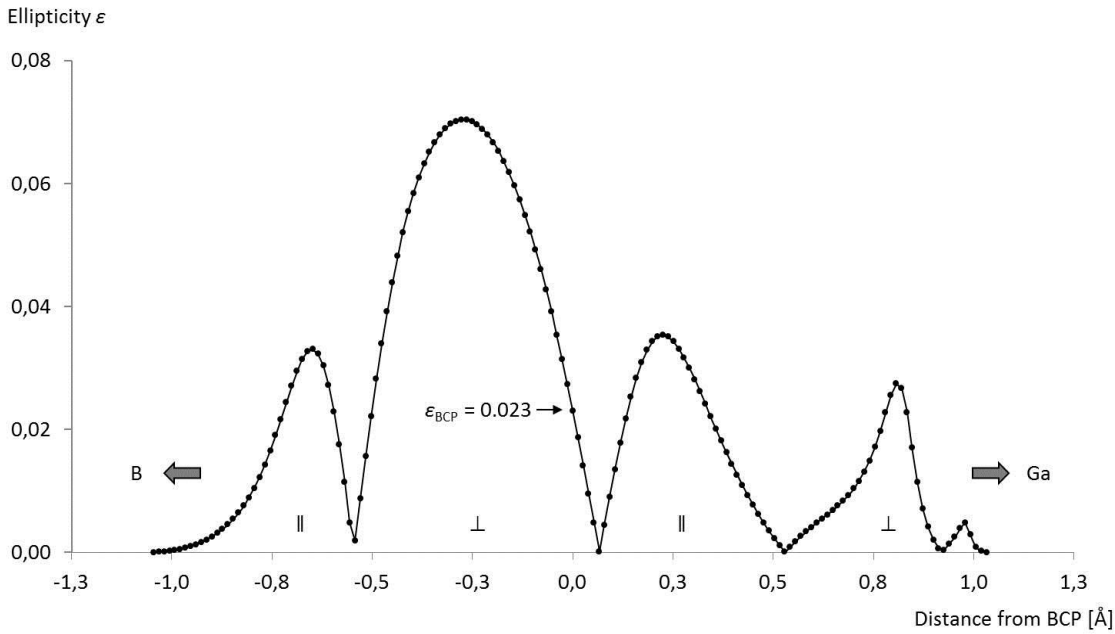

Figure S23. Bond ellipticity, ε, along the B−Ga bond in $[Me_2Ga\{B(NArCH)_2\}]$ (**2a**) (Ar = C_6H_3-2,6-*i*Pr_2). "⊥" and "∥" indicate that the major axis of the bond lies perpendicular to or in the molecular plane.

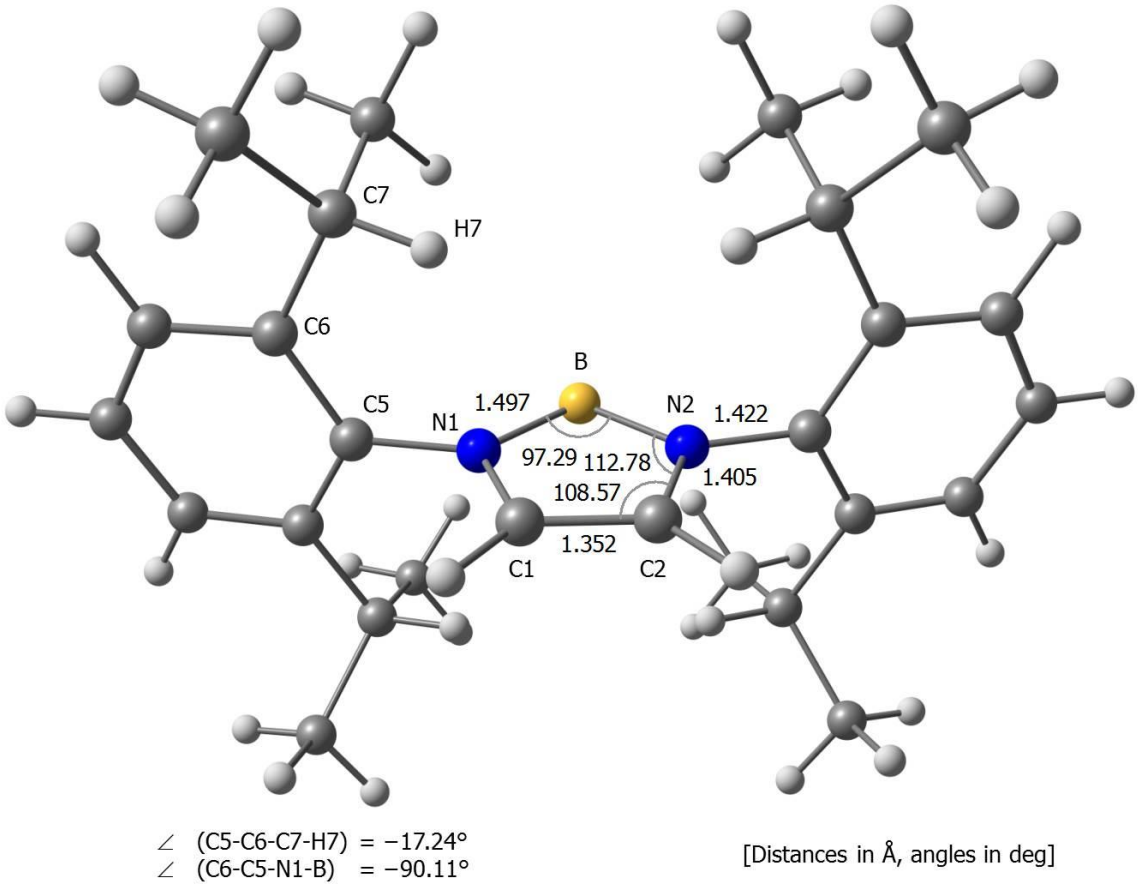

Figure S24. Optimized geometry (C_{2v} symmetry) and selected geometrical parameters for $[B(NArCH)_2]^-$ (**1a**) (Ar = C_6H_3-2,6-*i*Pr_2).

Cartesian Coordinates for **1a**:

6	-3.606073000	3.181477000	-0.912225000
6	-3.606073000	-3.181477000	-0.912225000
6	0.000000000	-0.676023000	-1.730471000
6	-2.551434000	2.466505000	-0.051327000
6	0.000000000	0.676023000	-1.730471000
6	-2.551434000	-2.466505000	-0.051327000
6	-3.073744000	2.185817000	1.370211000
6	-1.223889000	3.210405000	0.017700000
6	-1.200672000	4.582459000	0.286991000
6	-1.223889000	-3.210405000	0.017700000
6	3.606073000	-3.181477000	-0.912225000
6	-1.200672000	-4.582459000	0.286991000
6	0.000000000	-2.518019000	-0.118722000
6	0.000000000	2.518019000	-0.118722000
6	-3.073744000	-2.185817000	1.370211000

6	3.606073000	3.181477000	-0.912225000
6	0.000000000	5.269777000	0.417280000
6	0.000000000	-5.269777000	0.417280000
6	1.223889000	-3.210405000	0.017700000
6	1.200672000	-4.582459000	0.286991000
6	2.551434000	-2.466505000	-0.051327000
6	1.223889000	3.210405000	0.017700000
6	1.200672000	4.582459000	0.286991000
6	2.551434000	2.466505000	-0.051327000
6	3.073744000	-2.185817000	1.370211000
6	3.073744000	2.185817000	1.370211000
1	-4.501802000	2.558102000	-1.003876000
1	-3.228260000	3.380615000	-1.919595000
1	-3.228260000	-3.380615000	-1.919595000
1	-4.501802000	-2.558102000	-1.003876000
1	-3.918914000	4.136693000	-0.477181000
1	0.000000000	-1.348612000	-2.577447000
1	0.000000000	1.348612000	-2.577447000
1	-3.918914000	-4.136693000	-0.477181000
1	-2.346952000	1.498575000	-0.510762000
1	-2.346952000	-1.498575000	-0.510762000
1	-4.008914000	1.615133000	1.333093000
1	3.228260000	-3.380615000	-1.919595000
1	-2.136052000	5.120045000	0.405006000
1	3.228260000	3.380615000	-1.919595000
1	-4.008914000	-1.615133000	1.333093000
1	-2.136052000	-5.120045000	0.405006000
1	-3.265079000	3.120229000	1.910974000
1	3.918914000	-4.136693000	-0.477181000
1	4.501802000	-2.558102000	-1.003876000
1	3.918914000	4.136693000	-0.477181000
1	-2.333637000	1.599336000	1.921414000
1	-3.265079000	-3.120229000	1.910974000
1	0.000000000	6.335344000	0.627252000
1	0.000000000	-6.335344000	0.627252000
1	2.346952000	-1.498575000	-0.510762000
1	4.501802000	2.558102000	-1.003876000
1	-2.333637000	-1.599336000	1.921414000
1	2.136052000	-5.120045000	0.405006000
1	2.136052000	5.120045000	0.405006000
1	2.346952000	1.498575000	-0.510762000
1	4.008914000	-1.615133000	1.333093000
1	3.265079000	-3.120229000	1.910974000
1	3.265079000	3.120229000	1.910974000
1	2.333637000	-1.599336000	1.921414000
1	4.008914000	1.615133000	1.333093000
1	2.333637000	1.599336000	1.921414000
5	0.000000000	0.000000000	0.590605000
7	0.000000000	-1.123629000	-0.398457000
7	0.000000000	1.123629000	-0.398457000

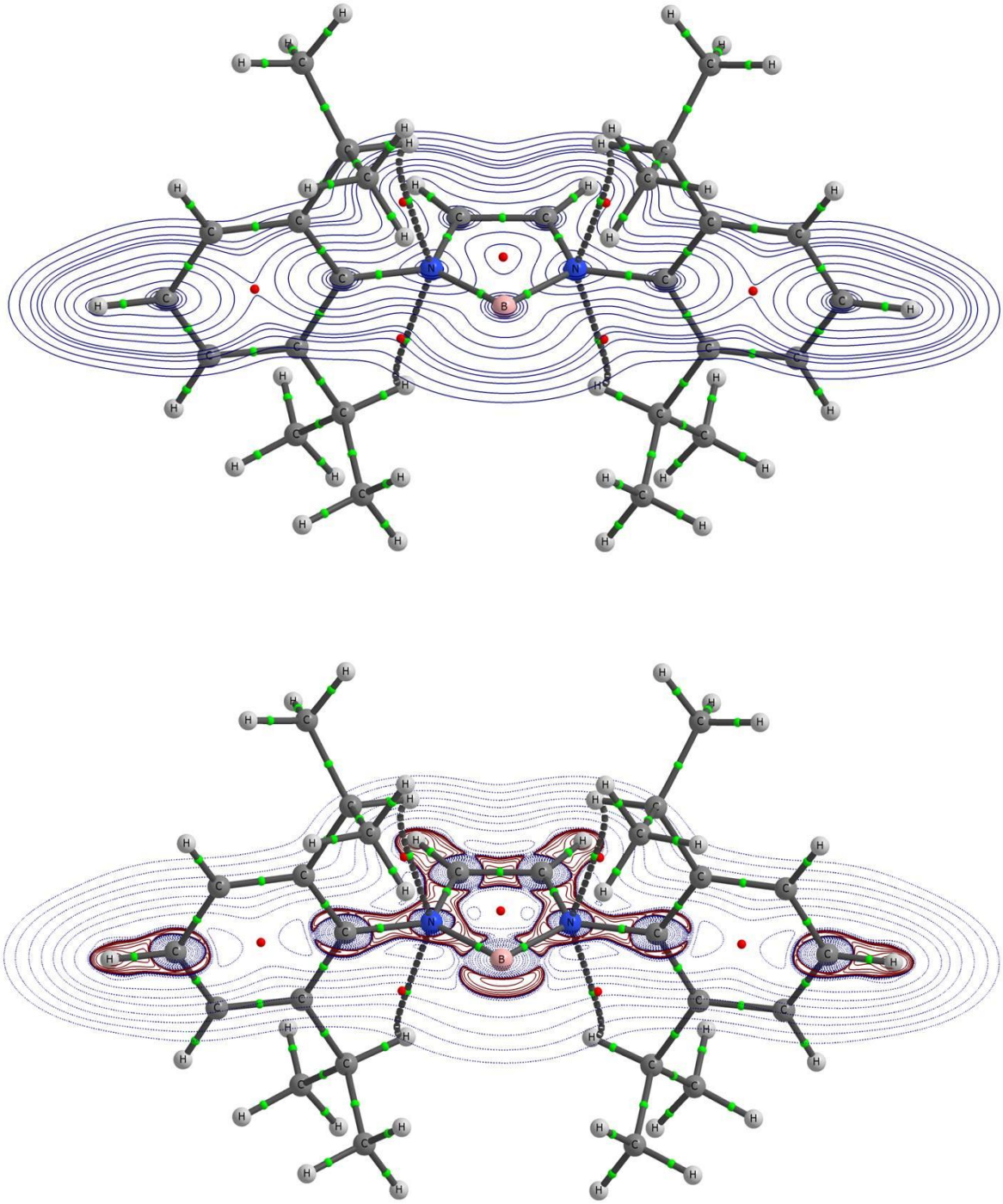

Figure S25. Contour plots of the electron density, $\rho(\mathbf{r})$, (top) and the negative Laplacian, $-\nabla^2\rho(\mathbf{r})$, (bottom) in the molecular plane of $[B(NArCH)_2]^-$ (**1a**) (Ar = C_6H_3-2,6-*i*Pr_2). Bond paths are superimposed; BCPs and RCPs are represented by green and red points, respectively. Dashed bond paths indicate weak C−H···N interactions; other BCPs with ρ_b < 0.01 e bohr^{-3} (C−H···H−C and C−H···B interactions) are not shown.

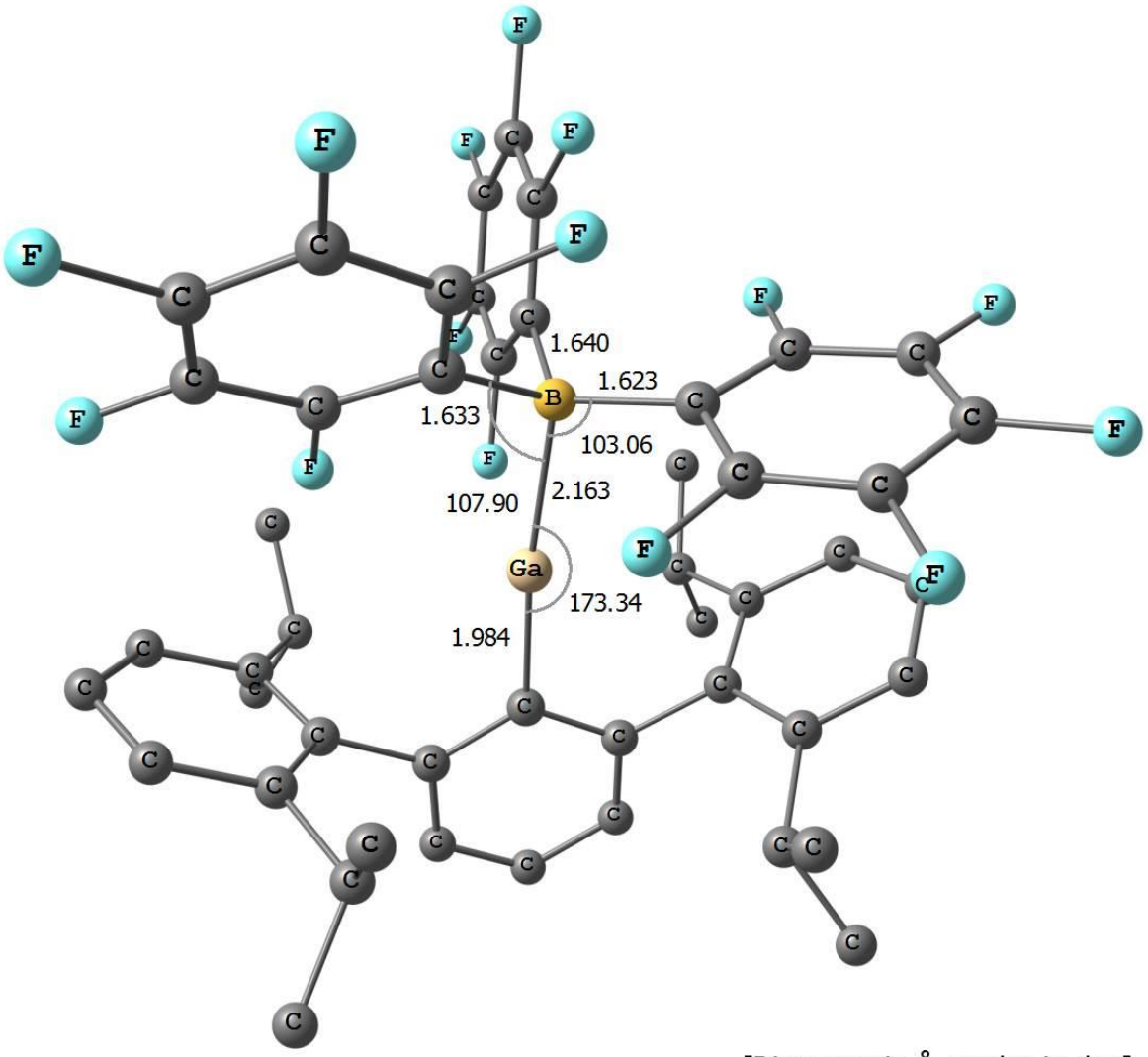

[Distances in Å, angles in deg]

Figure S26. Optimized geometry (C_1 symmetry) and selected geometrical parameters for [Ar′Ga{B(C_6F_5)$_3$}] (**C**) (Ar′ = C_6H_3-2,6-Dipp$_2$, Dipp = C_6H_3-2,6-*i*Pr$_2$). All hydrogen atoms are omitted for clarity.

6	1.296886000	-4.540641000	0.784649000
6	4.252231000	-2.415303000	-3.509325000
6	3.794764000	-0.769099000	-1.645493000
6	2.792098000	-2.257990000	0.124359000
6	4.612129000	0.309095000	-1.999224000
6	3.624350000	-1.069661000	-0.272769000
6	2.683167000	-4.613958000	0.691339000
6	5.257184000	1.068009000	-1.033407000
6	3.423798000	-3.485104000	0.354424000
6	4.276494000	-0.296671000	0.717721000
6	5.090312000	0.763344000	0.310812000
6	3.858013000	0.662570000	3.047678000
6	4.132523000	-0.598386000	2.208301000
6	5.369289000	-1.343968000	2.747105000
1	-4.751659000	-3.218217000	0.564575000
1	-3.533714000	-3.857879000	-1.477826000
1	-3.521067000	-2.672095000	2.619726000
1	-2.371720000	-3.484386000	-3.358023000
1	-2.119209000	-5.874860000	-2.211052000

1	-2.436008000	-2.042932000	4.434208000
1	-1.122679000	-2.276586000	-3.056877000
1	-0.751650000	-3.715150000	-4.008263000
1	-1.800037000	-0.760169000	3.406581000
1	-0.508658000	-5.979751000	-2.934509000
1	-1.657187000	-4.458641000	4.105856000
1	-0.713062000	-6.181918000	-1.188043000
1	1.871416000	-1.432953000	-4.488924000
1	1.514463000	-0.253698000	-3.225357000
1	-0.852189000	-1.356501000	4.776651000
1	0.197824000	-3.932810000	-1.751699000
1	2.926168000	-0.038197000	-4.259673000
1	0.159405000	-2.346562000	2.849533000
1	-0.119144000	-4.770963000	3.291771000
1	-0.146453000	-3.851394000	4.801346000
1	2.504954000	-2.343912000	-2.288185000
1	0.720412000	-5.427290000	1.022288000
1	3.793571000	-3.064163000	-4.261271000
1	4.951582000	-1.749423000	-4.022915000
1	4.753388000	0.552099000	-3.046163000
1	3.035584000	1.246678000	2.632198000
1	4.830057000	-3.042653000	-2.826138000
1	5.884379000	1.901664000	-1.327518000
1	3.273111000	-1.261665000	2.331806000
1	3.187422000	-5.557667000	0.867972000
1	3.592531000	0.383256000	4.070628000
1	4.501430000	-3.552295000	0.258067000
1	5.592968000	1.368392000	1.055932000
1	4.735922000	1.312072000	3.103404000
1	5.538767000	-2.281112000	2.212115000
1	5.244089000	-1.578159000	3.808499000
1	6.269662000	-0.731636000	2.641131000
5	-0.867899000	1.269607000	-0.127334000
9	-5.746712000	-0.991722000	-2.318490000
9	-5.674228000	-0.239535000	0.300873000
9	-3.508077000	-0.712675000	-3.862827000
9	-0.714283000	4.942960000	-3.606256000
9	-2.062861000	3.103032000	-2.230535000
9	-3.467904000	0.782213000	1.367410000
9	-2.365981000	3.606671000	0.700719000
9	-2.366749000	4.755723000	3.130581000
9	-1.253813000	0.282572000	-2.805987000
9	1.961604000	5.287498000	-3.224609000
9	-0.911684000	3.678107000	5.166372000
9	3.282156000	3.727300000	-1.412999000
9	1.946829000	1.836596000	-0.028171000
9	0.584851000	0.253440000	2.311888000
9	0.560070000	1.408458000	4.724299000
31	0.405031000	-0.472653000	0.018362000

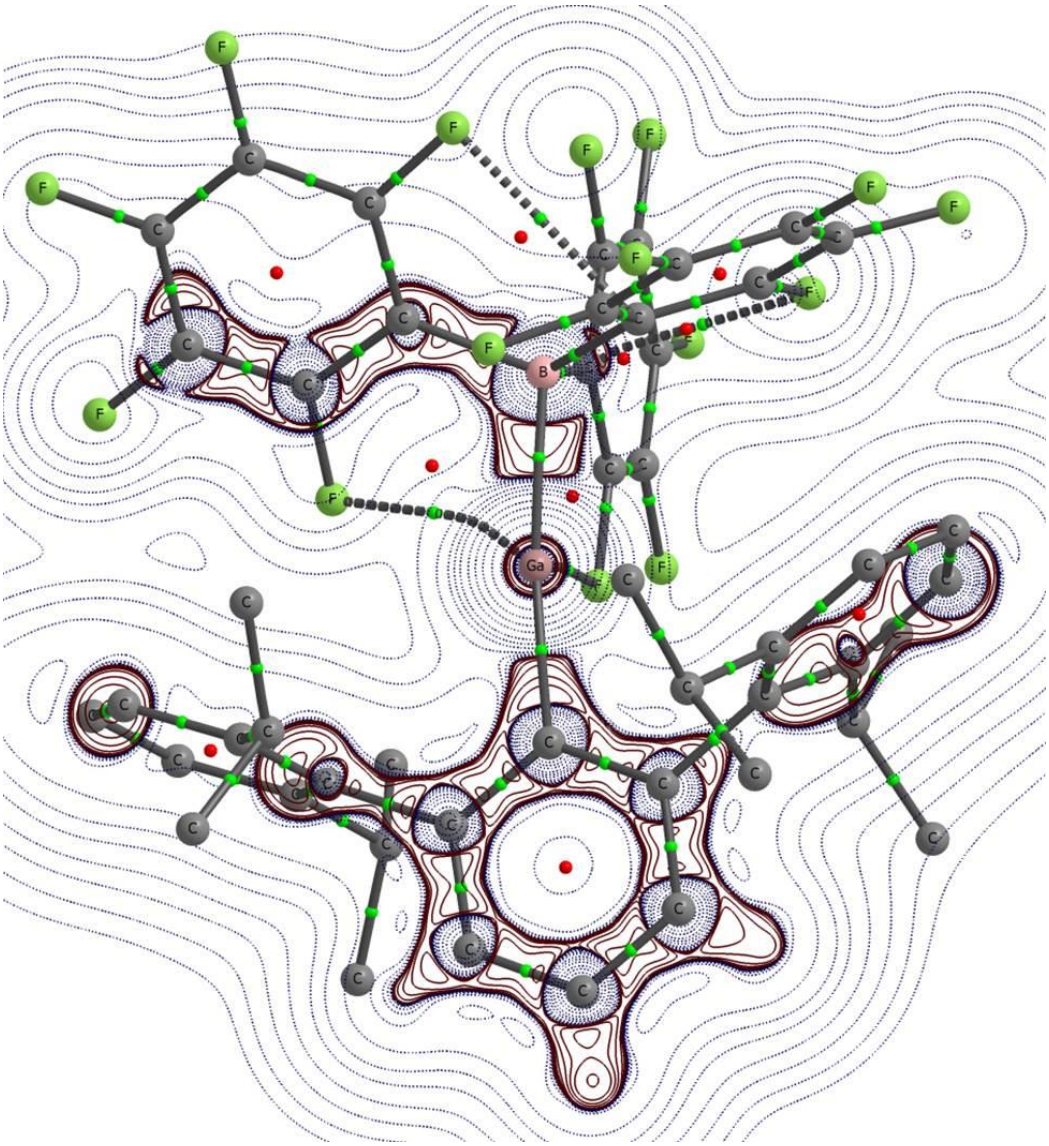

Figure S27. Contour plot of the negative Laplacian, $-\nabla^2\rho(\mathbf{r})$, in the molecular plane of [Ar′Ga{B(C_6F_5)$_3$}] (**C**) (Ar′ = C_6H_3-2,6-Dipp$_2$, Dipp = C_6H_3-2,6-*i*Pr$_2$). Bond paths are superimposed; BCPs and RCPs are represented by green and red points, respectively. All hydrogen atoms are omitted for clarity. Dashed bond paths indicate weak Ga···F and C···F interactions; further BCPs with ρ_b < 0.01 e bohr^{-3} (F···C, F···H, C−H···H−C, C···H interactions) are not shown.

Table S2. AIM charges (q) and selected topological parameters for the DFT-optimized systems [$Me_2Ga\{B(NArCH)_2\}$] (**2a**) (Ar = C_6H_3-2,6-*i*Pr_2), $[B(NArCH)_2]^-$ (**1a**) (Ar = C_6H_3-2,6-*i*Pr_2), and [Ar′$Ga\{B(C_6F_5)_3\}$] (**C**) (Ar′ = C_6H_3-2,6-$Dipp_2$, Dipp = C_6H_3-2,6-*i*Pr_2). Experimental distances are denoted in square brackets.

Moiety	d [Å]	ρ_b [eÅ^{-3}]	$\nabla^2\rho_b$ [eÅ^{-5}]	ε	H_b [hartree Å^{-3}]	G_b/ρ_b [hartree e^{-1}]	δ
[$Me_2Ga\{B(NArCH)_2\}$] **2a** [q(B) = +1.09; q(Ga) = +1.10; q(N) = −1.42; q(C)[a] = +0.33]							
B−Ga	2.095 [2.067(3)][b]	0.656	−0.817	0.02 (⊥)[c]	−0.321	0.40	0.78
Ga−C	2.000 [1.967][d]	0.733	+2.965	0.03 (∥)	−0.341	0.75	0.76
B−N	1.449 [1.436][d]	1.235	+12.109	0.01 (⊥)	−1.082	1.56	0.65
N−C	1.395 [1.395][d]	1.982	−18.630	0.16 (⊥)	−2.556	0.63	1.08
C−C[e]	1.355 [1.351(4)][b]	2.242	−23.239	0.38 (⊥)	−2.463	0.37	1.52
C−H···N	2.391 [2.46][b]	0.104	+1.461	2.80	+0.017	0.82	0.05
$[B(NArCH)_2]^-$ **1a** [q(B) = +0.76; q(N) = −1.38; q(C) = +0.27]							
B−N	1.497	1.070	+10.859	0.19 (∥)	−0.854	1.51	0.65
N−C	1.405	1.952	−18.452	0.17 (⊥)	−2.363	0.55	1.08
C−C[d]	1.352	2.246	−23.271	0.40 (⊥)	−2.478	0.38	1.55
C−H···N	2.379	0.108	+1.539	3.86	+0.017	0.84	0.05
[$\{C_6H_3Ar_2Ga\}B(C_6F_5)_3$] **C** [$q$(B) = +1.48; q(Ga) = +0.95]							
B−Ga	2.163 [2.124][f]	0.571	−1.999	0.01	−0.264	0.22	0.55
Ga−C	1.984 [1.949][f]	0.776	+2.447	0.07	−0.377	0.71	0.76
Ga−F	2.412 [2.413][f]	0.193	+2.257	0.19	−0.014	0.89	0.16
Ga···F	2.777 [2.697][f]	0.110	+1.098	0.62	0.000	0.70	0.08

[a] Carbon atoms in the boron containing heterocycle. [b] Experimental value, this work. [c] "⊥" or "∥" indicate that the major axis of the bond lies perpendicular to or within the molecular plane. [d] Average experimental value, this work. [e] C−C bond in the boron containing heterocycle. [f] Average experimental value, ref 16.

References:

(1) Stoe & Cie GmbH Darmstadt, Germany, **2009**.
(2) APEX v. 2012.10_0 Madison, WI, **2010**.
(3) Saint v. 7.99A Madison, WI, **2010**.
(4) Sheldrick, G. M., SHELXTL v. 2012.10_2, Madison, WI, **2012**.
(5) Sheldrick, G. M., SADABS v. 2012/1, Madison, WI, **2012**.
(6) L. J. Farrugia *J. Appl. Crystallogr.* **1997**, 565.
(7) POV-Ray v. 3.6 Williamstown, Victoria, Australia, **2004**, (http://www.povray.org).
(8) Hardman, N. J.; Power, P. P.; Gorden, J. D.; Macdonald, C. L. B.; Cowley, A. H. *Chem. Comm.* **2001**, 1866.
(9) Jutzi, P.; Neumann, B.; Reumann, G.; Schebaum, L. O.; Stammler, H.-G. *Organometallics* **2001**, *20*, 2854.
(10) M. J. Frisch; G. W. Trucks; H. B. Schlegel; G. E. Scuseria; M. A. Robb; J. R. Cheeseman; G. Scalmani; V. Barone; B. Mennucci; G. A. Petersson; H. Nakatsuji; M. Caricato; X. Li; H. P. Hratchian; A. F. Izmaylov; J. Bloino; G. Zheng; J. L. Sonnenberg; M. Hada; M. Ehara; K. Toyota; R, F.; J. Hasegawa; M. Ishida; T. Nakajima; Y. Honda; O. Kitao; H. Nakai; T. Vreven; J. A. Montgomery, J.; J. E. Peralta; F. Ogliaro; M. Bearpark; J. J. Heyd; E. Brothers; K. N. Kudin; V. N Staroverov; T. Keith; R. Kobayashi; J. Normand; K. Raghavachari; A. Rendell; J. C. Burant; S. S. Iyengar; J. Tomasi; M. Cossi; N. Rega; J. M. Millam; M. Klene; J. E. Knox; J. B. Cross; V. Bakken; C. Adamo; J. Jaramillo; R. Gomperts; R. E. Stratmann; O. Yazyev; A. J. Austin; R. Cammi; C. Pomelli; J. W. Ochterski; R. L. Martin; K. Morokuma; V. G. Zakrzewski; G. A. Voth; P. Salvador; J. J. Dannenberg; S. Dapprich; A. D. Daniels; O. Farkas; J. B. Foresman; J. V. Ortiz; J. Cioslowski; Fox, D. J., GAUSSIAN 09, Revision C.01; Gaussian, Inc.: Wallingford, CT, **2010**.
(11) (a) Becke, A. D. *J. Chem. Phys.* **1993**, *98*, 5648; (b) Lee, C.; Yang, W.; Parr, R. G. *Phys. Rev. B* **1988**, *37*, 785; (c) Miehlich, B.; Savin, A.; Stoll, H.; Preuss, H. *Chem. Phys. Lett.* **1989**, *157*, 200.
(12) (a) McLean, A. D. C., G. S. *J. Chem. Phys.* **1980**, *72*, 5639; (b) Krishnan, R. B., J.; Seeger, R.; Pople, J. A. *J. Chem. Phys.* **1980**, *72*, 650; (c) Binning, R. C.; Curtiss, L. A. *J. Comput. Chem.* **1990**, *11*, 1206; (d) McGrath, M. P.; Radom, L. *J. Chem. Phys.* **1991**, *94*, 511; (e) Curtiss, L. A. M., M. P.; Blaudeau, J.-P.; Davis, N. E.; Binning Jr., R. C.; Radom, L. *J. Chem. Phys.* **1995**, *103*, 6104.
(13) Keith, T. A., AIMALL (*Version 13.05.06*), TK Gristmill Software, Overland Park KS, USA, **2012** (aim.tkgristmill.com).
(14) Foster, J. P.; Weinhold, F. *J. Am. Chem. Soc.* **1980**, *102*, 7211.
(15) Zhurko, G. A., CHEMCRAFT (http://www.chemcraftprog.com).
(16) Hardman, N. J.; Wright, R. J.; Phillips, A. D.; Power, P. P. *J. Am. Chem. Soc.* **2003**, *125*, 2667.